Auckland
Regional Council
TE RAUHITANGA TAIAO

Hauraki regional harbour model : set-up calibration and verification

August 2004 TP238

Auckland Regional Council
Technical Publication 238, August 2004
ISSN 1175 205X ISBN 1-877353-52-3
Printed on recycled paper

Hauraki Regional Harbour Model: Set-up, Calibration and Verification

J. W. Oldman
A. Senior
R. Haskew
D. Ramsay

Prepared for
Auckland Regional Council

© All rights reserved. This publication may not be reproduced or copied in any form without the permission of the client. Such permission is to be given only in accordance with the terms of the client's contract with NIWA. This copyright extends to all forms of copying and any storage of material in any kind of information retrieval system.

NIWA Client Report: HAM2004-038
August 2004

NIWA Project: ARC04299

National Institute of Water & Atmospheric Research Ltd
Gate 10, Silverdale Road, Hamilton
P O Box 11115, Hamilton, New Zealand
Phone +64-7-856 7026, Fax +64-7-856 0151
www.niwa.co.nz

Contents

1	**Executive Summary**	**1**
2	**Introduction and background**	**3**
3	**Model setup**	**5**
3.1	Bathymetric grid setup	5
3.2	Simulation periods	6
3.3	Boundary conditions	6
4	**Model calibration**	**8**
4.1	Introduction	8
4.2	Tidal height calibration	8
4.2.1	Tide height constituent data	8
4.2.2	Time series data (Whitford)	12
4.2.3	Highest astronomical tide verification	15
4.3	Tidal current calibration	16
4.3.1	Tidal current constituent data	17
4.3.2	Tidal current time series calibration	18
4.4	Baroclinic calibration	28
4.4.1	Temperature – Firth of Thames	29
4.4.2	Salinity – Waitemata Harbour	30
5	**Schematic model runs**	**33**
5.1	Introduction	33
5.2	Model run details and results	33
6	**Conclusions**	**36**

7 References 37

8 Appendix 1 38

9 Appendix 2 39

Reviewed by:

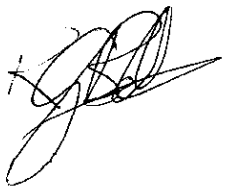

Dr Rob Bell

Approved for release by:

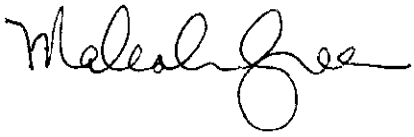

Dr Malcolm Green

Formatting checked

1 Executive Summary

This preliminary report describes the development, calibration, verification and initial application of the Hauraki Regional Harbour Model (RHM). The RHM has been developed by NIWA under contract to the Auckland Regional Council (ARC). The purpose of the RHM is to provide a consistent and reliable modelling framework for ARC and associated Territorial Local Authorities (TLAs) to help assess the impacts of discharges and catchment land-use changes on the receiving water and sediment quality of the harbours and waters of the inner Hauraki Gulf and associated harbours and estuaries.

Initial conclusions from the set-up, calibration and verification of the model include:

- A regional harbour model (RHM) has been set up for the inner Hauraki Gulf and associated harbours, to provide a consistent and reliable framework to assist future assessments of the environmental effects of discharges to the marine environment.
- The RHM has been calibrated and verified against appropriate available field data. This process has included comparing model predictions of tidal water levels, tidal currents and temperature stratification, against actual field measurements.
- Calibration and verification of tidal levels provided a very good match between observed and predicted water levels across the entire model domain.
- Calibration and verification of tidal currents ellipses and currents provided a reasonable match between observed and predicted. Calibration of tidal currents is generally more difficult because current velocities vary spatially much more than the more slowly changing tidal water levels. Consequently, obtaining a good match between modelled current velocities and field measurements is much more dependent on the spatial grid resolution of the model. For example, for the RHM comparisons are between field measurements collected at a particular location, depth, and time whereas model predictions are for currents averaged over time, distance and depth (i.e. 100m by 100m grid cells in the horizontal and 2m depth layers). Calibration of tidal currents (and dispersal models which suffer the same constraints) normally improves considerably by using a higher resolution model grid that reflects the spatial variation of the current velocity and mixing processes being modelled. This is achieved using a nested model grid within the RHM centred on the specific area of interest.
- Calibration of the dispersal model for large-scale plumes and mixing behaviour has shown that temperature variations due to thermal mixing of oceanic (i.e. outer Gulf) and estuarine waters (i.e. Firth of Thames) are predicted well by the model. In combination, advection, horizontal and vertical mixing processes are well represented within the model. The mixing of catchment-derived freshwater inflows to the Waitemata Harbour and saline waters of the inner Gulf are also being modelled accurately, further confirming the ability of the dispersion model to simulate the mixing processes at length scales of 100 m or more.

- A series of initial baseline tide, wind and stratification scenarios have been run to provide a baseline dataset for future use of nested models within the RHM. Nested models need to be at a 1:3 ratio of 100 m (i.e. 33 m, 11 m grid cells). These higher-resolution nested models will provide a closer match to point-velocity measurements and small-scale plume behaviour than the baseline 100 m model.

This report will be supplemented by a RHM user manual to help guide the ARC and TLAs on the use, application, limitations and restrictions of the model (Ramsay et al., 2004). The user manual will include details of the metadatabase that is being developed to hold information on relevant field and model data. A further report (Oldman et al., 2004) will detail a demonstration project of the application of the RHM.

2 Introduction and background

Auckland Regional Council (ARC) is in the process of evaluating resource consent applications from network operators and territorial authorities for stormwater discharges into the marine receiving environment.

To assist with the assessment of both the near and far-field environmental effects of discharges to the marine environment, such as from stormwater and combined wastewater outfalls, ARC have commissioned the development of a hydrodynamic and water quality model. This model, known as the Hauraki Regional Harbour Model (RHM) has been developed for the inner Hauraki Gulf and associated harbours and estuaries, from Kawakawa Bay in the south through to Waiwera in the north (Figure 1).

Figure 1:
RHM model coverage and bathymetry of the inner Hauraki Gulf showing major harbours and estuaries along the Auckland Regions coastline.

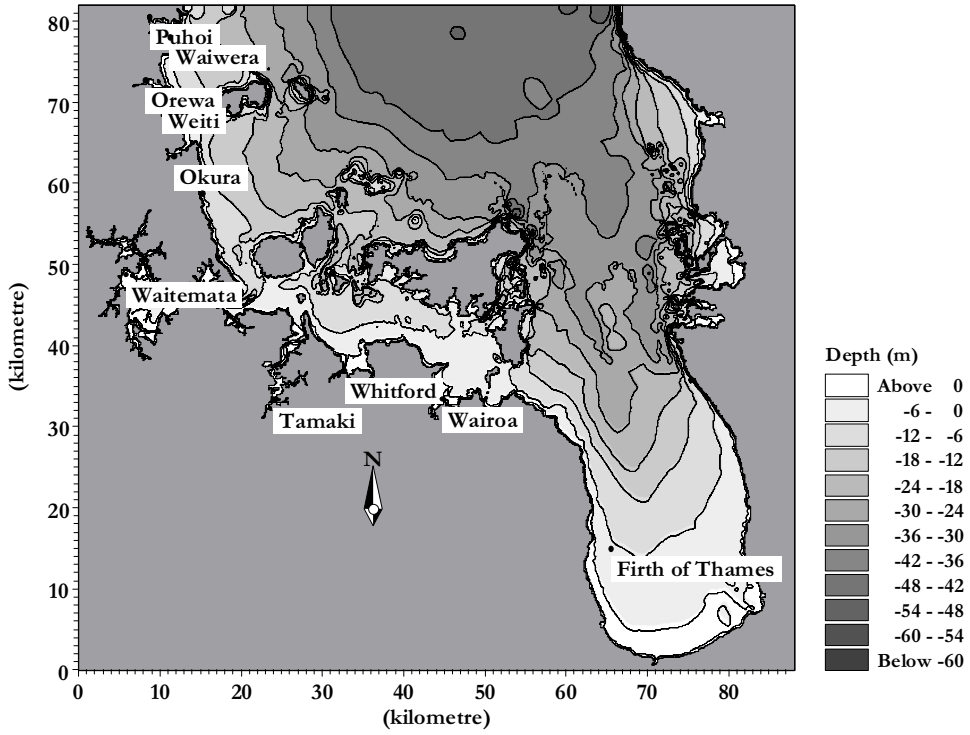

The overall purpose of the RHM is to provide a consistent and reliable framework to assist the Council, relevant Territorial Authorities and other associated parties to:

- Assess the impacts of discharges and catchment land-use changes on the receiving water and sediment quality of the harbours and waters of the inner Hauraki Gulf;
- Help inform the decision-making process with respect to capital expenditure priorities for stormwater and sewer networks.

This draft report outlines the development of the RHM its calibration and verification against existing tide, current and water column data. This report will be supplemented by a RHM user manual to help guide the ARC and TLAs on the use, application, limitations and restrictions of the model (Ramsay et al, 2004). The user manual will include details of the metadatabase that is being developed to hold information on relevant field and model data. A further report (Oldman et al, 2004) will detail a demonstration project of the application of the RHM.

The RHM model has been developed using the MIKE 3 suite of hydrodynamic and water quality models developed by DHI Water & Environment www.dhisoftware.com.

3 Model setup

3.1 Bathymetric grid setup

Existing bathymetric data held by NIWA was incorporated into the bathymetric database. Gaps in the database were identified and extra digitising (from relevant charts) was carried out for the Tamaki Strait. The final bathymetric database used to create the 100 m by 100 m grid is shown in Figure 2. The northern limit of the RHM was set to NZMG 6438500 (Cape Colville – Puhoi River). To simplify the model boundary conditions the model domain was extended south and east to include the whole of the Firth of Thames. The limits for the model domain are shown in Table 1.

Table 1:

Limits of the RHM domain.

Model Cell	NZMG		WGS-84	
	Easting (m)	Northing (m)	Latitude (°N)	Longitude (°E)
Lower left cell centre	2652000	6438000	-37.24930	174.59718
Upper right cell centre	2740000	6520000	-36.49170	175.56199

Figure 2:
RHM model domain limits (NZMG) and depth data points used to develop 100 m RHM grid.

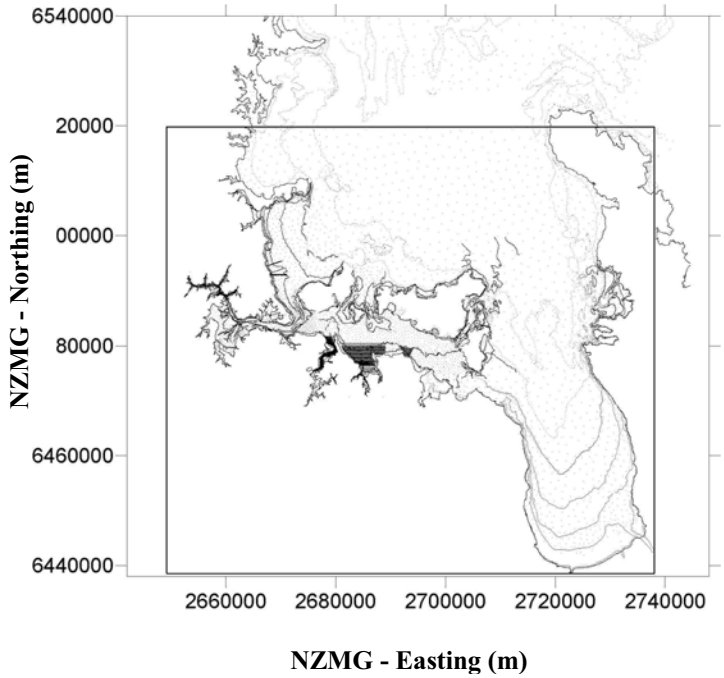

3.2 Simulation periods

The calibration and verification of the RHM, described in this report, involved running the model over the same time periods as previously collected field data within the model area, and comparing how well the particular parameters simulated in the model compared with the measured field data. Within the calibration and verification, the model was run over the following periods, using the field data listed in Table 2.

Table 2

Summary of data used and simulation periods during the RHM calibration and verification

Period	Data type	Data measurement location	Reference (if relevant)
4 weeks	Tide heights	Whangaparoa Ports of Auckland Waiheke (West) Waiheke (East) Coromandel Harbour Tararu	Black et al. (2000)
21st November to 21st December, 2000	Tide heights	Pine Harbour Marina	Senior et al. (2003)
1st April to 14th May 1992	Tidal current measurements	Red Bluff	Water Quality Centre (1992)
21st November to 10th December 2000	Tidal current measurements	Whitford embayment	Senior et al. (2003)
March 2000	Water column temperature	Firth of Thames	Zeldis (Pers. Com.)
September 1999	Water column temperature	Firth of Thames	Zeldis (Pers. Com.)

3.3 Boundary conditions

Tidal boundary conditions were extracted from a calibrated tidal model of New Zealand's EEZ (Walters et al., 2001). This larger tidal model has been calibrated against measurements from the sea-level network including a number of sites within the Hauraki Gulf (Marsden Point, Mokohinua Islands and Auckland) and is the basis of NIWA's tide forecasting service.

Figure 3 gives the time-series of predicted tides during April/May 1992 at the northern boundary of the RHM. During mean tides (tide range ~2.7 m) the slope along the northern boundary reaches 15 cm around 2 hours after high water. During spring tides (tide range ~2.8 m) the slope peaks around 18 cm and during neap tides (tide range ~2.3 m) the slope along the northern boundary peaks around 10 cm (Figure 3a). On the rising tide, water levels at Cape Colville are lower than those at Puhoi River while on the falling tide the water levels at the eastern end of the boundary are generally higher than those at the western end (Figure 3b).

Figure 3:
Time-series of levels at western end of northern boundary (Puhoi) and the slope along the northern boundary (Cape Colville – Puhoi) for: (a) 1 April to 14 May 1992 and (b) close up of 22 April 1992.

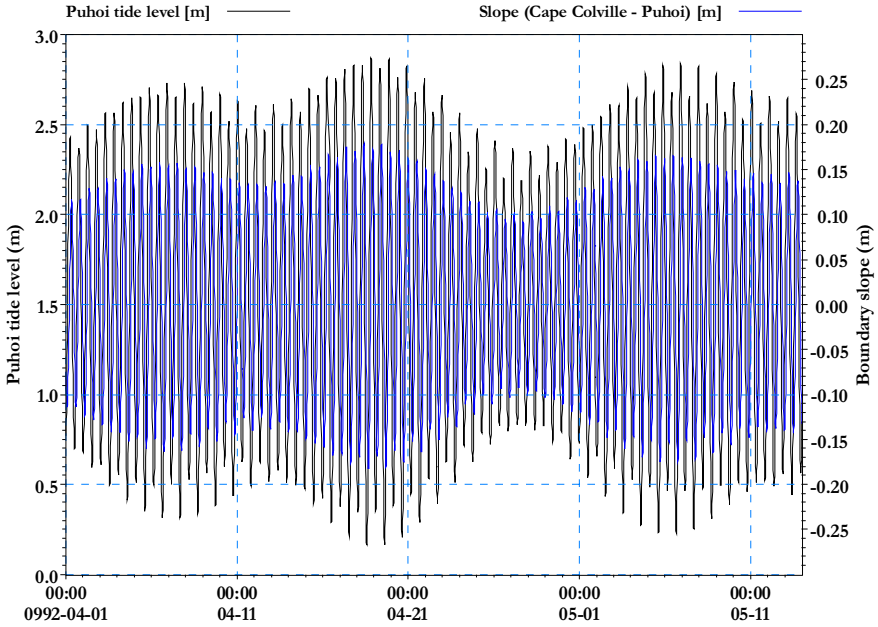

(a)

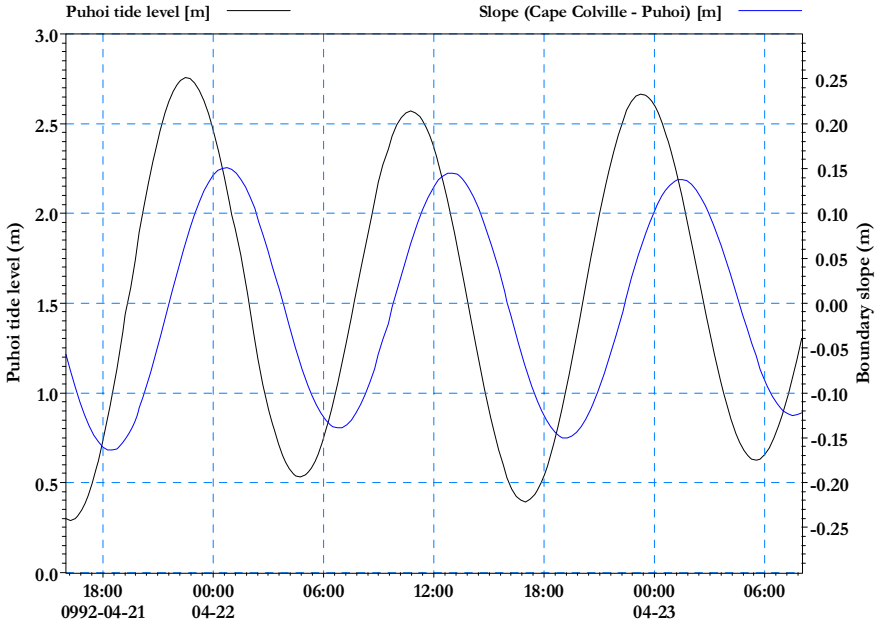

(b)

4 Model calibration

4.1 Introduction

Calibration is a process of adjusting parameters within the numerical model to achieve the best fit between observed and modelled data. Verification of the model is then done by carrying out further simulations to determine if the model is capable of predicting the various physical parameters over different time periods and different background conditions.

Spatial variation of tide heights occurs over kilometre or greater scale, with tidal periods ranging from hours up to days. When using a model grid resolution of 100 m, calibration of tidal heights is therefore relatively easy as tide heights tend not vary much over the resolution of the model. Calibration of tidal velocities is however more difficult because over the resolution of the model there can by large gradients (both in the horizontal and vertical) in measured velocities. Tidal velocities can also change very quickly in time. Thus the averaging of the model (both in time and more importantly space) limits the accuracy with which any numerical model of this type can predict tidal velocities. For similar reasons the calibration of dispersal is also difficult as it is common to have sharply varying gradients spatially (e.g. freshwater plume) that are very transient in time. Accuracy of both hydrodynamic and dispersal models are improved by using a model grid resolution that reflects this spatial variation (be it tidal velocities or dispersal). Increased model grid resolution is achieved using nested model grids within the RHM that are centred on the specific areas of interest.

4.2 Tidal height calibration

The first step in calibrating a model is to check that the specified boundary conditions and bathymetry give a good match between observed and predicted water levels inside the model domain.

4.2.1 Tide height constituent data

The RHM was run for a period of 4 weeks using tidal boundary conditions from the EEZ model (Walters et al., 2001). From this run the amplitude (half range) and phase (timing of high water) of the three main twice–daily tides M2, S2 and N2 were extracted and compared to tide gauge data. A good calibration of tide propagation can only be achieved if the schematised bathymetry within the model accurately represents the bathymetry of the area being modelled. Good schematisation of the bathymetry ensures that the tidal prisms (the volume of water exchanged between high and low water) can accurately simulated leading to the correct amplification of tidal heights. Calibration of tide constituent is achieved primarily through adjusting the bed resistance within the model until the best match is achieved between the modelled tide heights and measurements. Other model parameters such as the user

selected flooding and drying depths, turbulence model selection and the eddy viscosity do not significantly alter the calibration of tide heights. Within a depth-averaged (2-D) model the bed resistance is defined as

$$\frac{g\,u\,|u|}{C^2} \tag{1}$$

where g is gravity (m^2/s) , u is the velocity (m/s) and C is the Chezy number ($m^{1/3}/s$). Within the three-dimensional MIKE3 model the bed resistance is defined as

$$C_D\,u^*|u^*| \tag{2}$$

where C_D is the drag coefficient and u^* is the first computational velocity encountered above the bed. C_D is defined by the assuming a logarithmic profile between the seabed and the first computational velocity node, thus

$$C_D = \left[\frac{1}{\kappa}\log\left(\frac{z}{k_s/30}\right)\right]^{-2} \tag{3}$$

where κ is the von Karman's constant (0.41) , z is the distance between the seabed and the first computational point (m), and k_s is the bed roughness length scale (m).

The best calibration against field data (all three major tidal constituents) was achieved by setting the Chezy roughness (C) value to 25 or the bed roughness scale (k_s) to 0.04. Use of a higher bed resistance (either a Chezy value lower than 25 or a k_s greater than 0.04) resulted in predicted tidal ranges smaller than those observed. Conversely applying a lower bed resistance gave tide ranges that were too high. Tables 3 to 5 indicate that the model provides good predictions of tidal constituents across the RHM domain. Model results for Tararu in the southern Firth of Thames show the largest differences with observations. This error could be minimised by applying a spatially varying resistance (i.e. define a resistance coefficient at each cell within the model) if it was considered that the discrepancy was significant in terms of the level of accuracy needed within the Firth of Thames area. Figures 4 to 6 gives the spatial plot of the tidal range for the three major tidal constituents.

Table 3:

Twice-daily lunar M_2 tide height calibration[1].

Location	Observed		Modelled		Difference	
	Amplitude (m)	Phase (^{o}NZST)	Amplitude (m)	Phase (^{o}NZST)	Amplitude (m)	Phase[2] (^{o}NZST)
Whangaparaoa	1.03	208	1.02	201	-0.01	-7
Ports of Auckland	1.16	204	1.1	210	-0.06	6
Waiheke (West)	1.02	198	1.08	204	0.06	6
Waiheke (East)	1.16	202	1.08	204	-0.08	2
Coromandel Harbour	1.01	206	1.14	202	0.13	-4
Tararu	1.27	204	1.22	220	-0.05	16

Table 4:

Twice-daily solar S_2 tide height calibration.

Location	Observed		Modelled		Difference	
	Amplitude (m)	Phase (^{o}NZST)	Amplitude (m)	Phase (^{o}NZST)	Amplitude (m)	Phase (^{o}NZST)
Ports of Auckland	0.191	273	0.182	265	0.009	8
Waiheke (West)	0.180	265	0.160	262	0.020	3
Waiheke (East)	0.188	260	0.160	262	0.028	-2
Coromandel Harbour	0.189	264	0.165	265	0.024	-1
Tararu	0.195	269	0.170	271	0.025	-2

Table 5:

Twice-daily elliptical lunar N_2 tide height calibration.

Location	Observed		Modelled		Difference	
	Amplitude (m)	Phase (^{o}NZST)	Amplitude (m)	Phase (^{o}NZST)	Amplitude (m)	Phase (^{o}NZST)
Ports of Auckland	0.234	180	0.190	182	0.034	-2
Waiheke (East)	0.230	173	0.180	170	0.050	3

[1] Note: Amplitude is the half-range and the phase, expressed in degrees of a full cycle, defines when the high water occurs for that tide.
[2] For example, phase difference of 1° for the M_2 tide = 2 minutes difference in timing of high water.

Figure 4:
Tide-height amplitude (half-range) calibration for M_2 across the RHM domain.

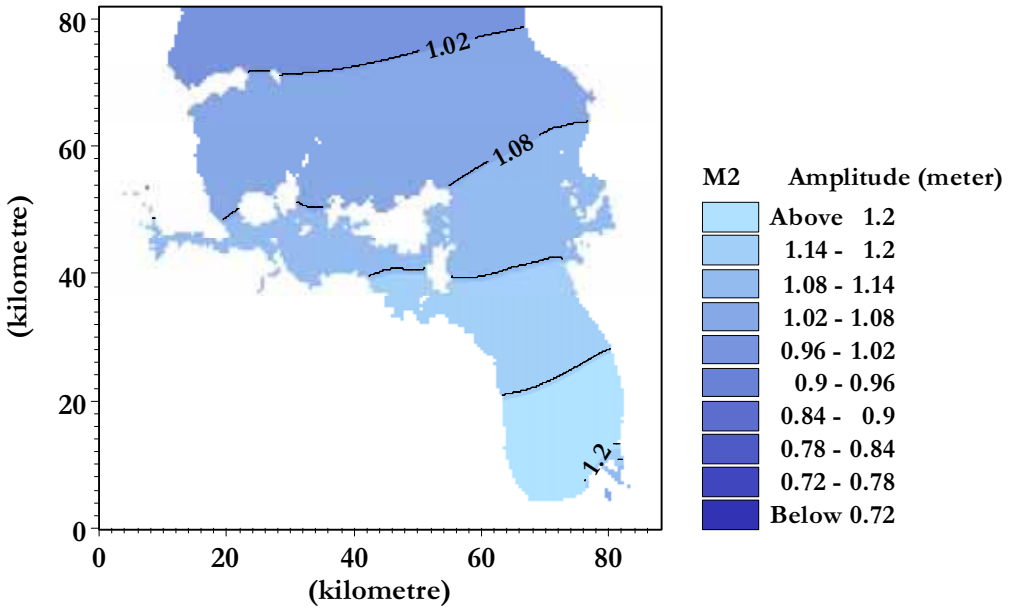

Figure 5:
Tide-height amplitude (half-range) calibration for S_2 across the RHM domain.

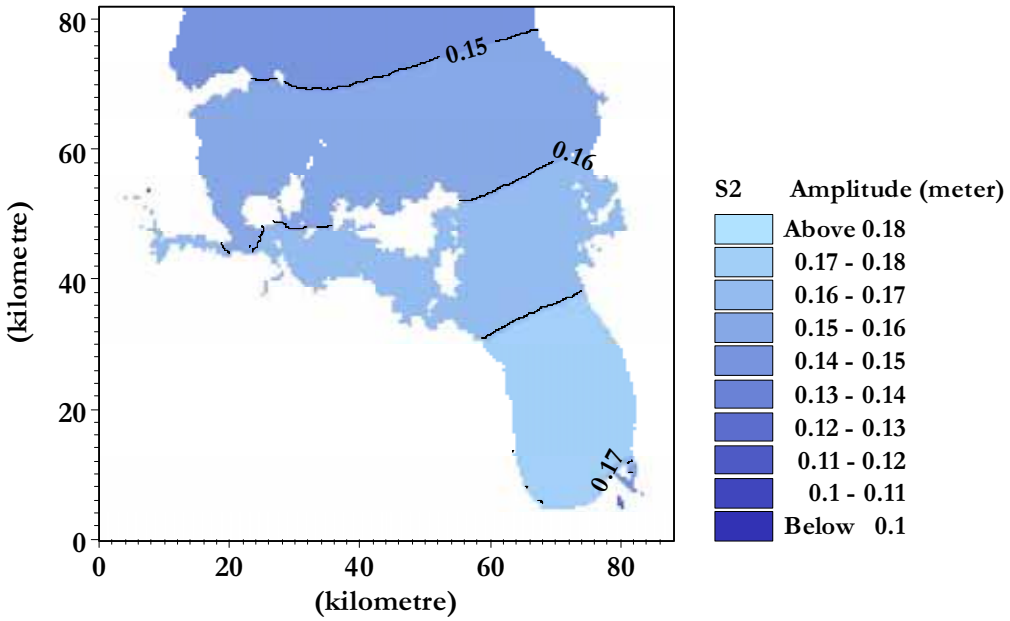

Figure 6:
Tide-height amplitude (half-range) calibration for N_2 across the RHM domain.

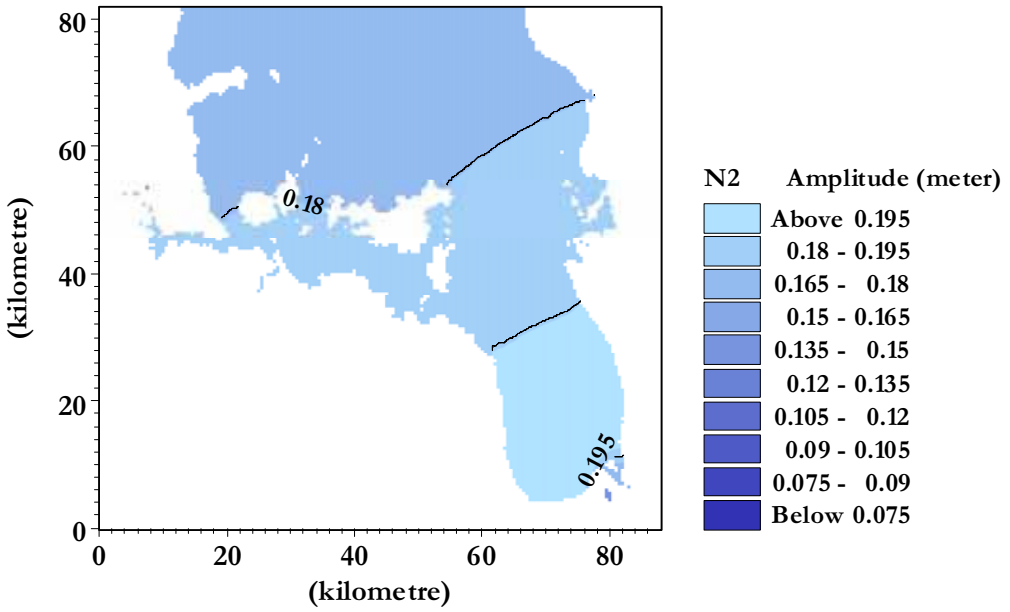

4.2.2 Time series data (Whitford)

In the previous section model results and field data are compared to determine if the tidal constituents are accurately simulated. The analysis of both the model and field data removes any non-tidal signal to derive the tidal constituent data. To determine if the model can also accurately model the effects of winds on water levels model data for a specified period is compared to field data – both the field and model data contain the non-tidal wind effects on water levels. Figures 7 to 9 show the measured and predicted water levels at Pine Harbour Marina for the period between the 21st of November 2000 and 21st of December 2000. The measured tides were not processed and so contain the tidal signal (i.e. the signal due to the astronomical tide) and the non-tidal signal (due to storm-surge, wind set-up barometric pressure gradients across the Gulf). Overall there is a good fit (r^2 =0.97, slope =0.997) between the measured and predicted water levels within the Whitford embayment (Figures 10).

For the period between the 25th and 26th of November (Figure 7), and between the 11th and 14th of December (Figure 9) the model is under-predicting the spring tidal range. During these times there were relatively high winds (8-12 m/s) from alongshore (330° True for the 25-26th November) or offshore (100° for the period between the 11th and 14th of December). This magnitude wind would produce a difference between the predicted (astronomical) and actual sea levels at the northern boundary. This difference propagates through the Gulf producing storm tides3 that are higher than the predicted high tide simulated by the tide-only version of the model. To improve the fit between the predicted and measured tides an adjustment could be made to the boundary

3 Storm-tide is the addition of a storm-surge height (arising from meteorological effects) to the predicted tide for that day.

condition for those particular days to account for storm-tide. Two methods could be used. The first would be to take measured pressures across the model domain and interpolate these onto each model cell. In this case the variations in atmospheric pressure are accounted for within the numerics and the boundary water levels are adjusted by the following formula;

$$Water\ level = Boundary\ condition - \frac{\left(P - P_{neutral}\right)}{\rho g} \qquad (4)$$

where P is the observed barometric pressure $P_{neutral}$ is the average atmospheric pressure, g is 9.8 m^2/s and is the water density.

Another approach would be to adjust the predicted model boundary condition by adding the observed difference between the predicted and measured water levels from a sea-level record (e.g., data from the Mokohinau Island sea-level gauge) during the time of interest. This method would take into account both barometric effects and wind set-up. Once again, if it was deemed necessary to improve the calibration of the model for a particular event or meteorological condition both these methods could be used to minimise the differences between the observed and predicted water levels on any particular day of interest. A summary of the percentage fit for the various calibration data is presented in Appendix 1.

Figure 7:
Predicted (black line) and measured (grey line) tide levels at Pine Harbour marina between 22nd November – 30th November 2000.

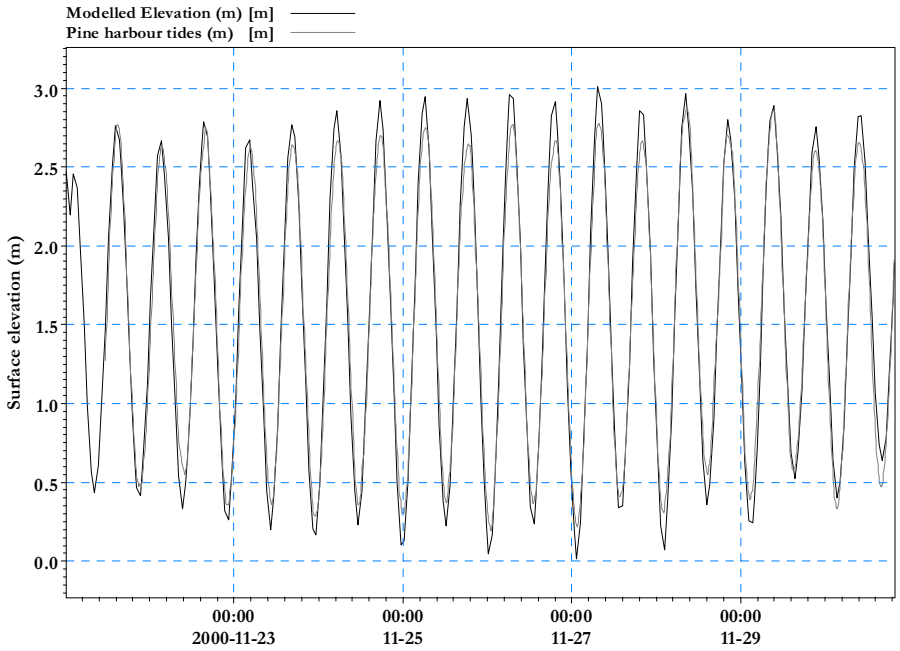

Figure 8:

Predicted (black line) and measured (grey line) tide levels at Pine Harbour marina between 1st December – 10th December 2000.

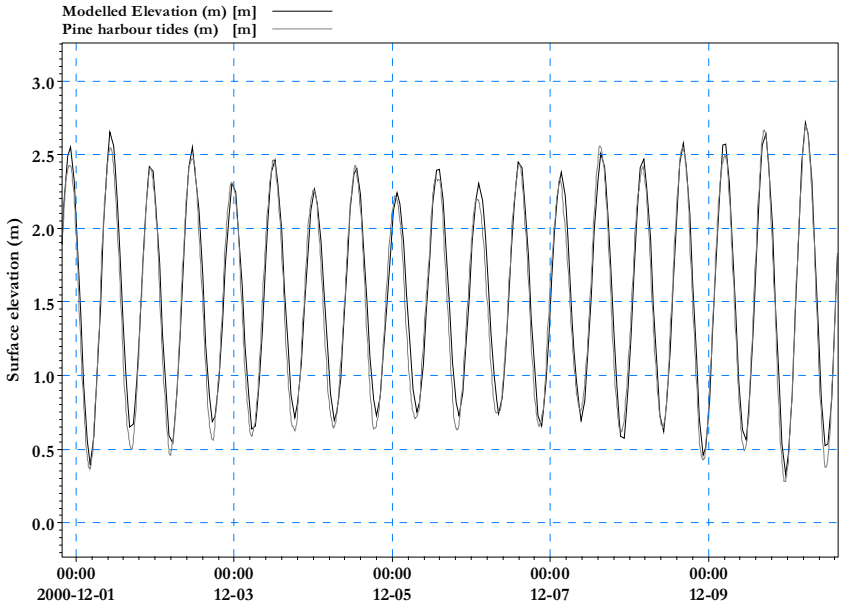

Figure 9:

Predicted (black line) and measured (grey line) tide levels at Pine Harbour marina between 11th December – 20th December 2000.

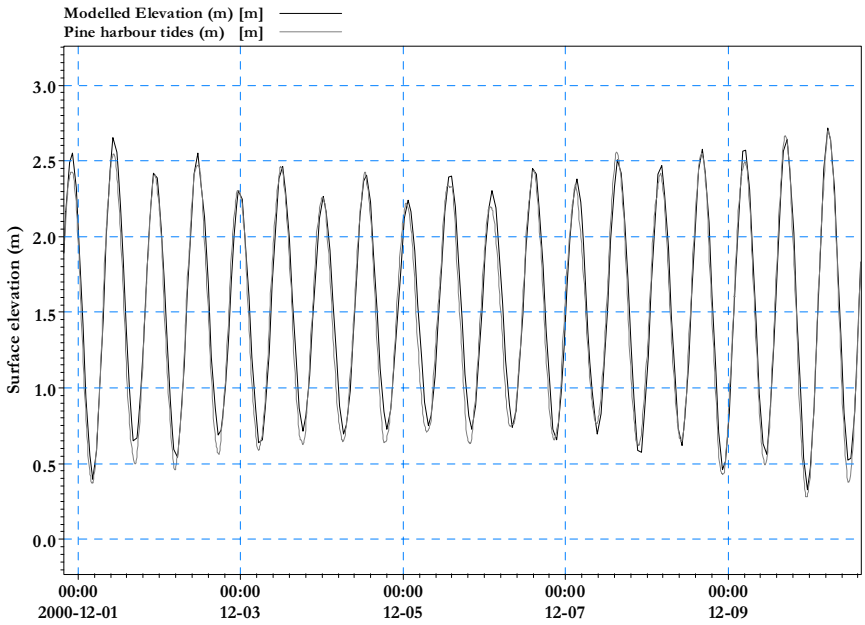

Figure 10:
Regression plot of predicted water levels within the Whitford embayment versus those observed between 22nd November 2000 – 20th December 2000. Note: these water levels include metrological effects on tides, which were not fully accounted for in the open-sea boundary forcing applied in the model simulation.

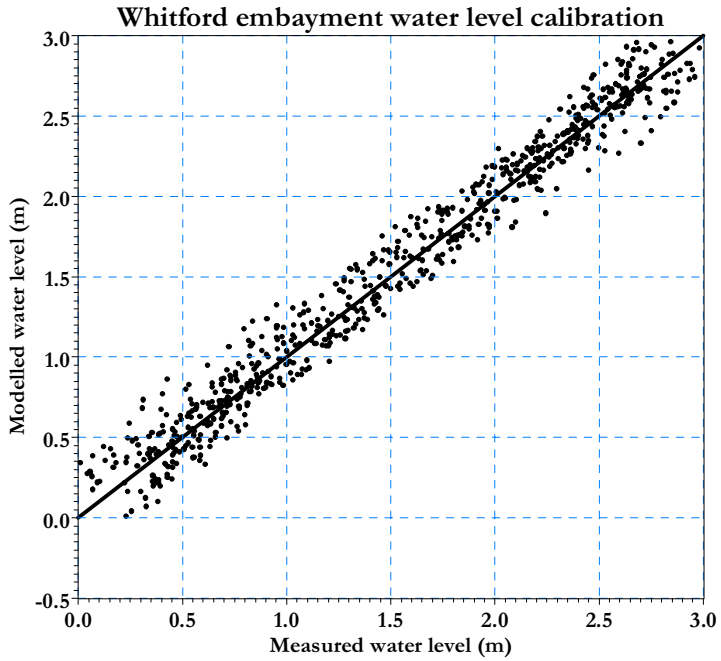

4.2.3 Highest astronomical tide verification

As part of the schematic model runs (see later section) a simulation of highest astronomical tide or HAT (tide range obtained from the coincidence of 13 tidal constituents) was carried out under calm (wind) conditions. No account was taken of barometric gradients across the model domain.

The bed resistance coefficients were left unaltered from the calibration, so this HAT simulation acts as a verification of the models performance across the full range of tide levels. The average tide range along the northern boundary for the HAT simulation was 3.26 m (low water 0.03 m, high water 3.29 m). Validation of the tide height calibration was obtained from this run for HAT values at Port of Auckland, Tararu, and East Coast Bays and are summarised in Table 5. The spatial plot of HAT is shown in Figure 11. Comparison with the three sites in Table 6 suggests the modelled HAT in the inner Gulf should have an additional 3-5 cm added.

Figure 11:
Modelled HAT across the whole of the RHM domain showing calibration sites for Ports of Auckland, East Coast Bays and Tararu.

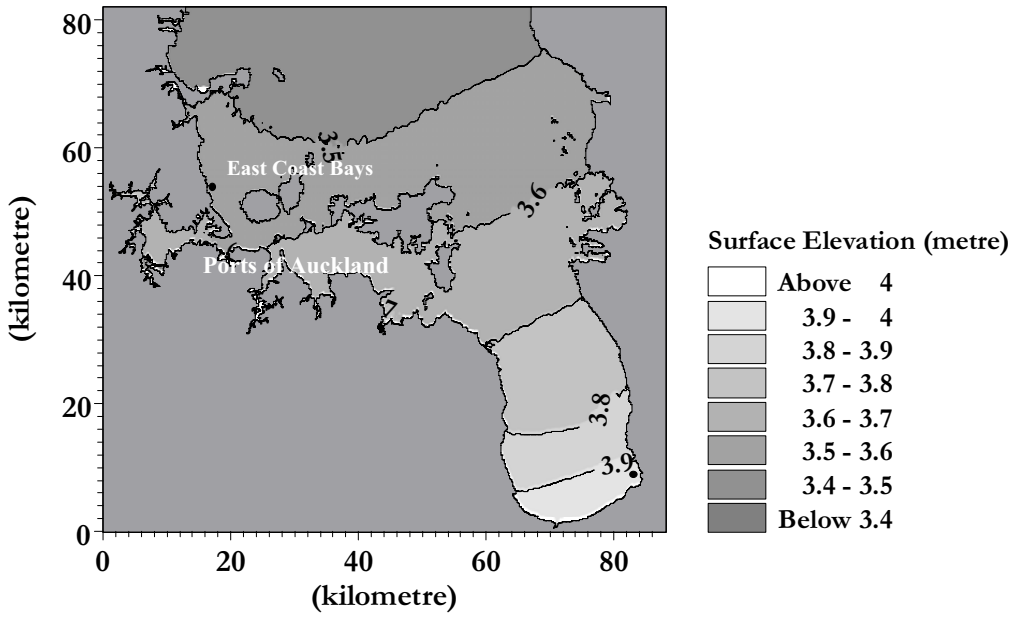

Table 6:

Verification of tide height calibration against HAT values.

Site	Observed HAT (m)	Modelled HAT
Port of Auckland	3.65	3.60
East Coast Bays	3.55	3.52
Tararu	4.01	3.95

4.3 Tidal current calibration

Having established that the model can accurately simulation the rise and fall of the tide across the RHM domain the next step in the calibration process is to check if the predicted tidal currents match observed data. This is done by comparing model predictions against observed tidal current ellipse data and time-series tidal current data at selected locations.

4.3.1 Tidal current constituent data

There are a total of 4 sites within the RHM domain where tidal current ellipse data have been observed. During a full tidal cycle, the tidal current every hour represented by a current velocity vector (scalar arrow) will trace out an ellipse as shown on the left hand side of Figure 12. This ellipse can be represented as shown in the figure on the right hand side of Figure 12. In the extreme, where the tidal current is tightly confined in a channel, the ellipse may become a straight line (i.e. ebbing and flooding).

Figure 12:
Hourly tidal current velocity vectors (left) and tidal ellipse representation (right).

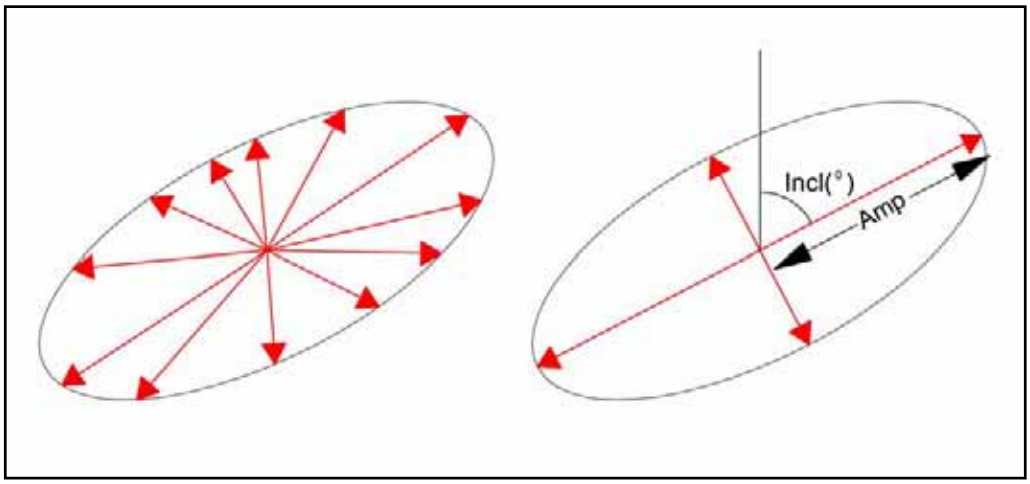

The following tables present the observed and modelled ellipse data. Note: Amp = maximum tidal current; Incl = inclination angle of the peak tidal current direction relative to True North; and Pha = the phase in degrees of the timing of the peak tidal current relative to NZST.

Table 7:

Calibration of tidal ellipses for M_2 currents.

Location	Observed			Modelled			Difference		
	Amp (m/s)	Incl (° True)	Pha (° NZST)	Amp (m/s)	Incl (° True)	Pha (° NZST)	Amp (m/s)	Incl (°)	Pha (°)
Red Bluff A	0.15	-17	288	0.12	-7	297	-0.03	10	9
Red Bluff B	0.18	7	298	0.16	5	297	-0.02	-2	-1
ECB (outer)	0.19	-1	294	0.18	-3	298	-0.01	-2	4
ECB (deep)	0.13	8	285	0.15	7	298	0.02	-1	13

Table 8:

Calibration of tidal ellipses for S_2 currents.

Location	Observed			Modelled			Difference		
	Amp (m/s)	Incl (° True)	Pha (° NZST)	Amp (m/s)	Incl (° True)	Pha (° NZST)	Amp (m/s)	Incl (°)	Pha (°)
Firth of Thames[4]	0.035	343	356	0.031	345	358	0.004	-2	-2
	0.045	351	352				0.014	-7	-6
	0.034	341	352				0.003	-4	-6
Whangaparoa	0.020	41	0	0.018	36	3	0.002	5	-3
ECB (deep)	0.026	15	1	0.021	4	353	0.005	9	-8

Table 9:

Calibration of tidal ellipses for N_2 currents.

Location	Observed			Modelled			Difference		
	Amp (m/s)	Incl (° True)	Pha (° NZST)	Amp (m/s)	Incl (° True)	Pha (° NZST)	Amp (m/s)	Incl (°)	Pha (°)
Firth of Thames	0.044	341	270	0.040	341	271	0.004	0	-1
	0.044	347	274				0.004	6	3
	0.042	342	269				0.002	2	-2
Whangaparoa	0.016	24	272	0.018	21	265	-0.002	3	7
ECB (deep)	0.041	1	280	0.031	355	274	0.010	-6	6

4.3.2 Tidal current time series calibration

A further check of the ability of the model to predict currents is to compare a time-series of measured currents against model predictions. As for the tidal height calibration no account was taken of metrological conditions to derive the northern boundary conditions i.e. the northern boundary for this simulation is an astronomical tide only. A model run was carried out for a period when two current meters were deployed at Red Bluff. Winds from the Mokohinau Islands AWS and the predicted tides along the northern boundary of the RHM were input to the model for the period from the 1st of April 1992 through to the 15th of May 1992. The wind rose for the period of the deployment is shown in Figure 13. Because this period contains a wide range of wind speeds and directions this simulation is a good test of the model in terms of its ability to predict currents under a range of tidal and wind conditions.

[4] Three values come from three separate current meter records at the same mooring.

Figure 13:
Wind rose from observed winds at Mokohinau Islands during the Red Bluff current meter deployment 1st of April 1992 through to the 15th of May 1992

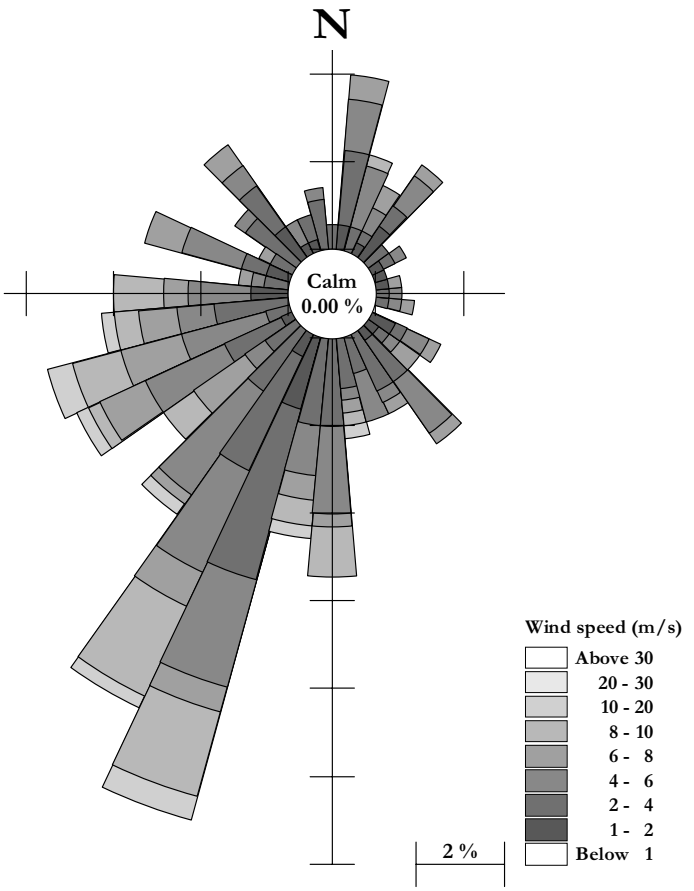

Figures 14 to 16 show the predicted currents at the Red Bluff sites for the simulation. The phasing and amplitude of the predicted currents is close to the observed for the majority of the simulation. The regression between the measured and predicted currents (Table 10) is shown in Figure 17. Occasionally the model under-predicts peak currents. The observed data comes from instruments 4.5 m above the bed in 10.0 m of water (Red Bluff A) and 4.0 m above the bed in 8.0 m of water (Red Bluff B) and so represent measurements at a fixed depth above the bed, a fixed point in space, and averaged over two minutes. The model output represents the average value within the relevant model depth layer (Figure 18) and over an entire 100 by 100 m grid cell at a particular time-step. Given the broader resolution of the RHM grid it is a reasonable predictor of currents (tidal and wind driven) at these sites.

Figure 14:

Time-series of predicted and measured currents at (a) Red Bluff A (inshore) and (b) Red Bluff B (offshore) between 1st of April 1992 and 11th of April 1992.

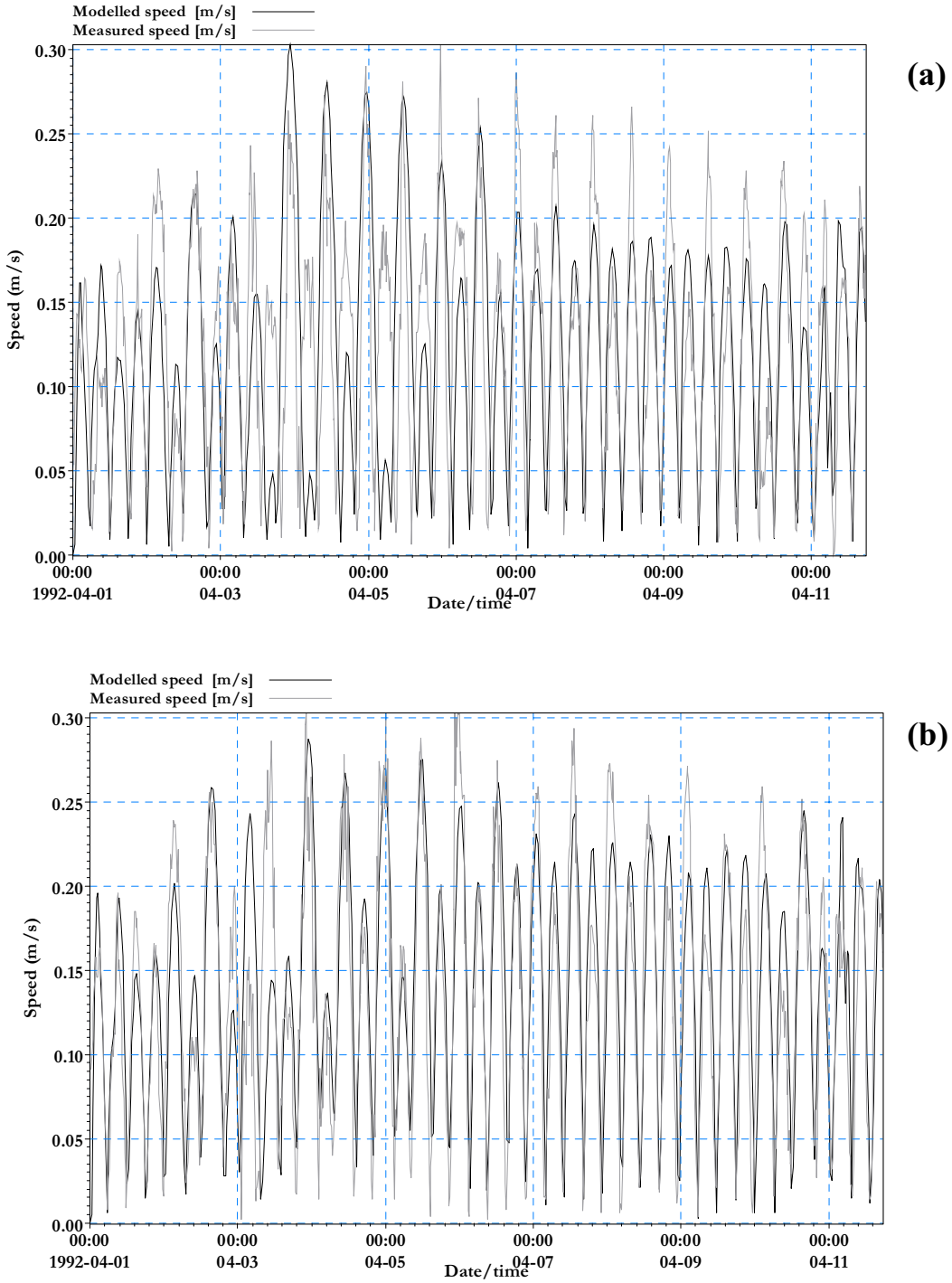

Figure 15:

Time-series of predicted and measured currents at (a) Red Bluff A and (b) Red Bluff B between 12th of April 1992 and 22nd of April 1992.

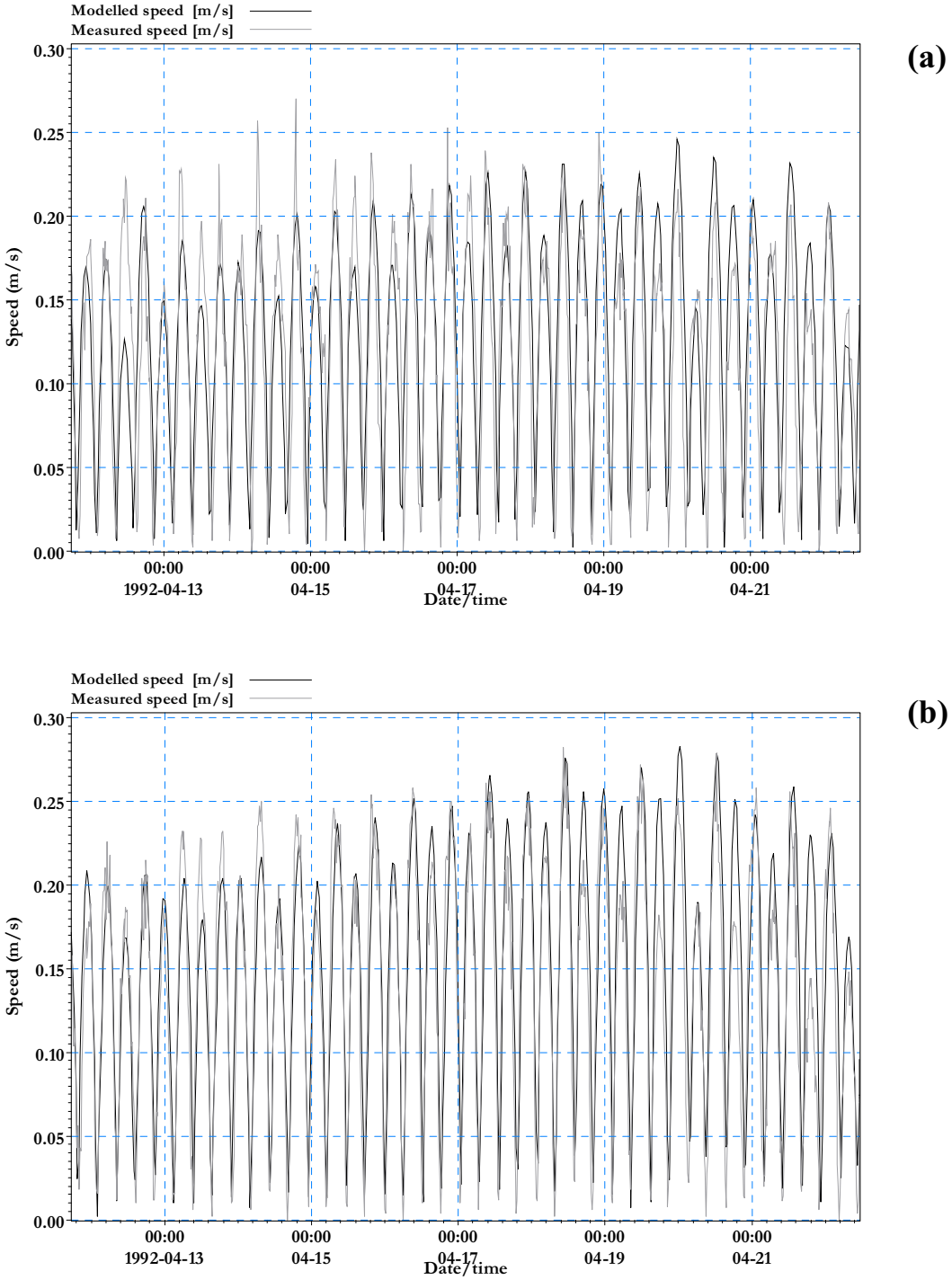

Figure 16:

Time-series of predicted and measured currents at (a) Red Bluff A and (b) Red Bluff B between 23rd of April 1992 and 30th of April 1992.

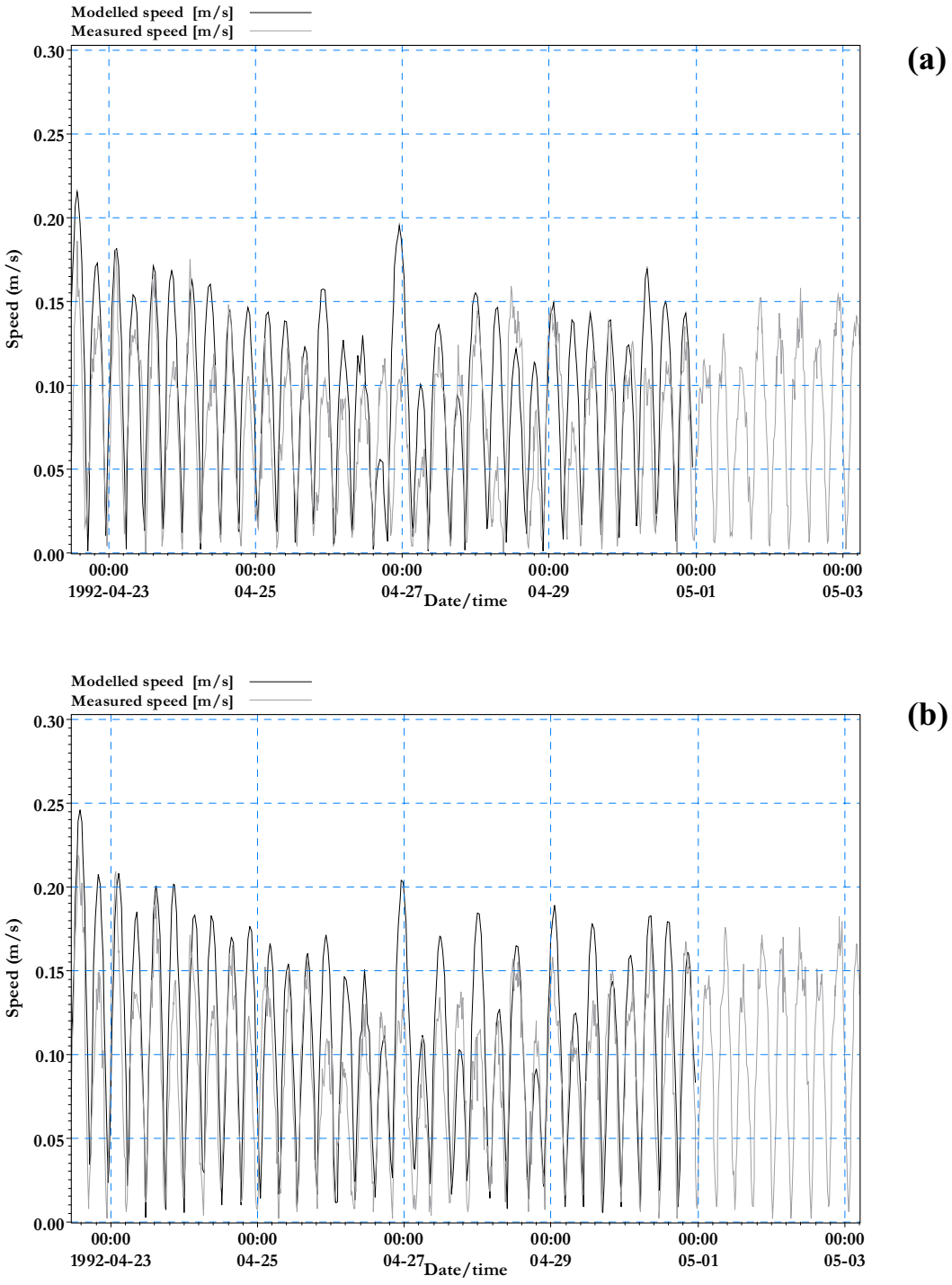

Figure 17:
Regression plot of predicted and measured current velocities at (a) Red Bluff A (inshore site) (b) and Red Bluff B (offshore site).

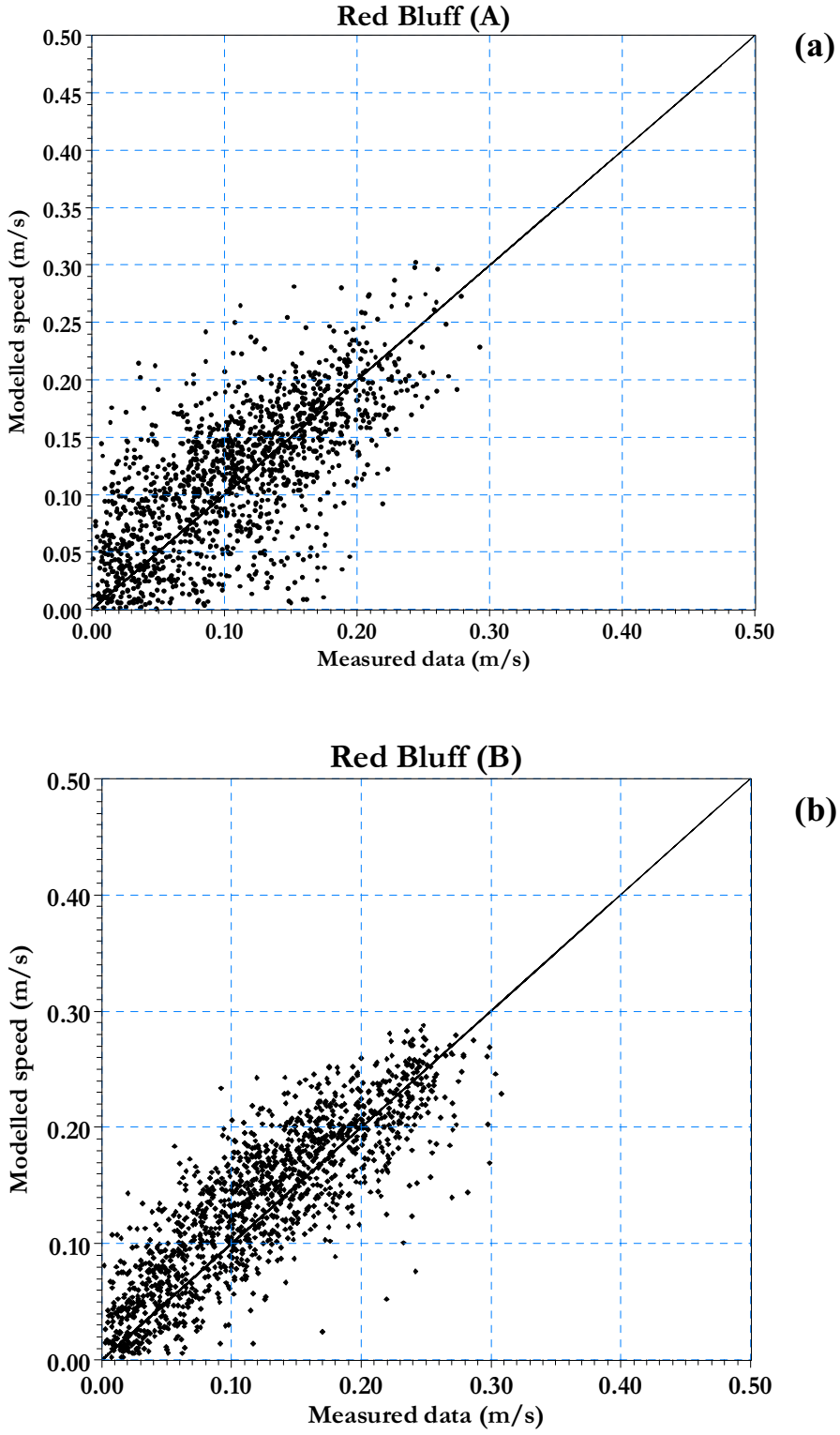

Verification of the models ability to predict currents come from a second model run carried out over the period between the 21st of November 2000 and the 10th of December 2000 corresponding to measured tidal current data collected within the Whitford Embayment including Cockle Bay to the north of Mangamangaroa Inlet. Figures 19 to 21 show that the measured speeds are higher than those predicted by the model but the phasing is good. Given the 100 m by 100 m cell schematisation of the bathymetry within the Whitford embayment this, is still a reasonable result. However, the regression between the measured and predicted currents, (Table 10 and Figure 22), show that the model is consistently under-predicting currents. Because of the schematisation of both the depth layering and bathymetry in the 100 by 100 m RHM grid, there are times when the model predicts close to zero speed whereas the measured currents at a point rarely drop below 0.05 m/s.

Given the broader scale resolution of the RHM grid it can be considered that the 100m grid is an adequate predictor of tidal and non-tidal currents. However, much improved calibration of the modelled current velocities can be expected for higher-resolution nested models within the RHM domain, as the grid resolution reduces towards a narrower area around the current-meter site. A summary of the percentage fit for the various calibration data is presented in Appendix 1.

Table 10:

Regression values for Red Bluff and Whitford current meter speeds versus model predictions (based on Figures 17 and 22).

	r^2	Intercept	Slope
Red Bluff A (inshore)	0.470	0.043	0.680
Red Bluff B (offshore)	0.725	0.035	0.823
Whitford	0.844	0.038	1.057

Figure 18:
Schematisation of the water column into depth layers within MIKE3.

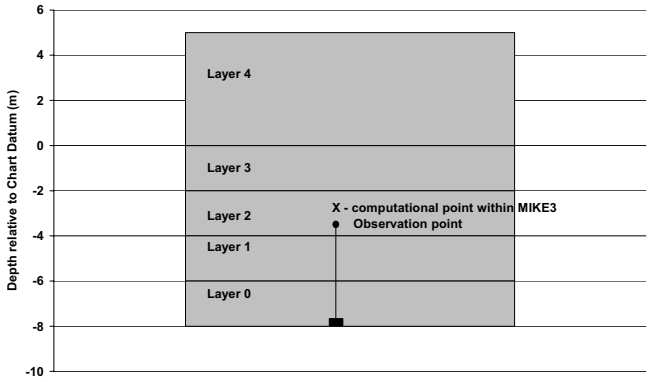

Figure 19:

Time-series of predicted and measured currents at Cockle Bay between (a) 15th and 19th of November 2000 (b) and 19th and 23rd of November 2000.

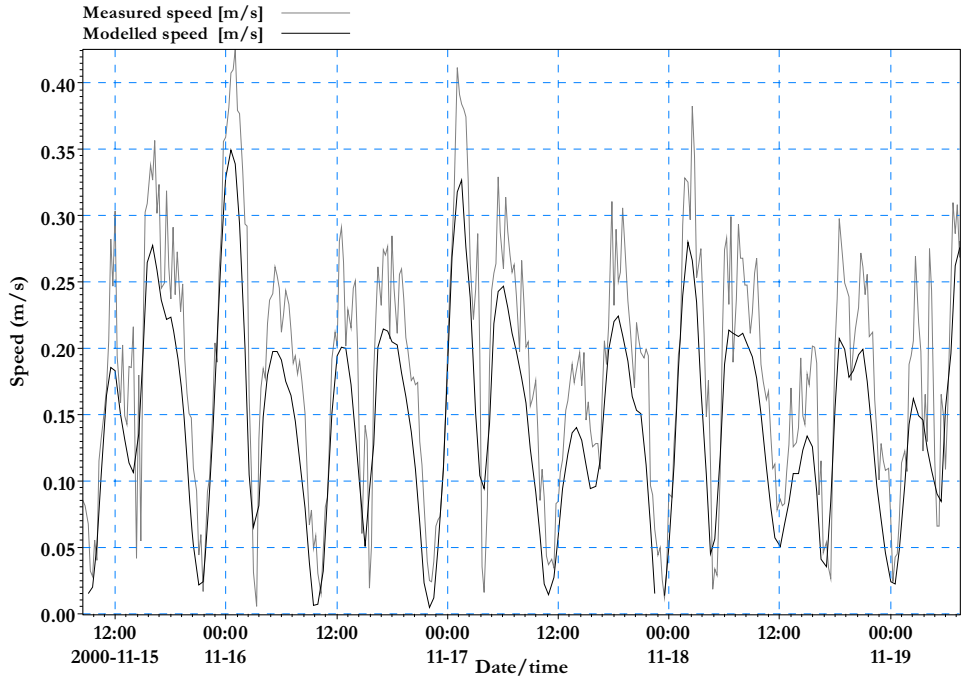

(a)

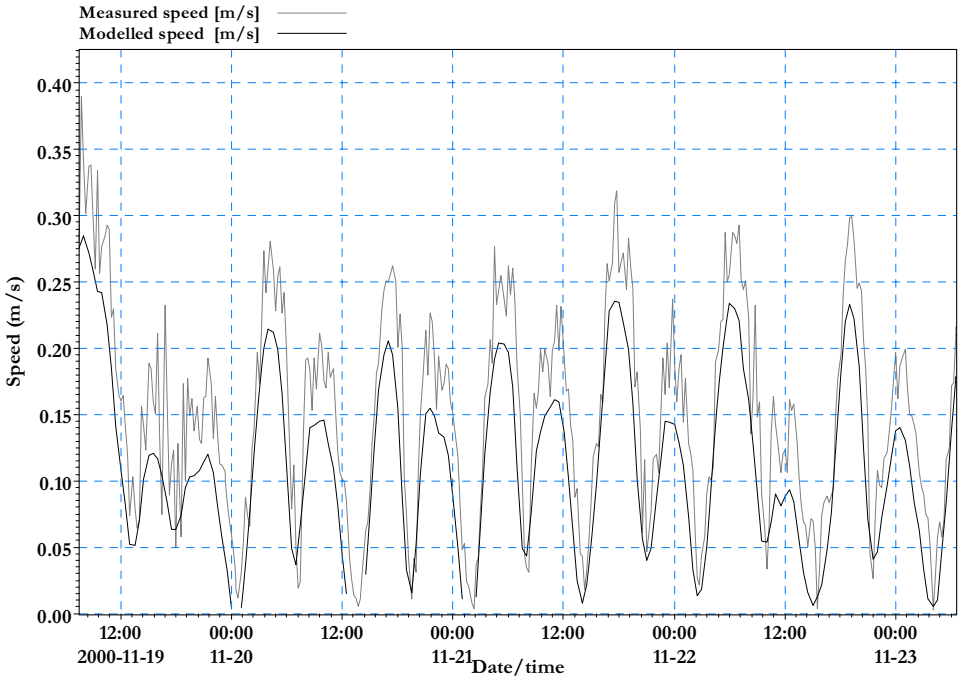

(b)

Figure 20:

Time-series of predicted and measured currents at Cockle Bay between (a) 23th and 27th of November 2000 (b) and 27th of November and 1st December 2000.

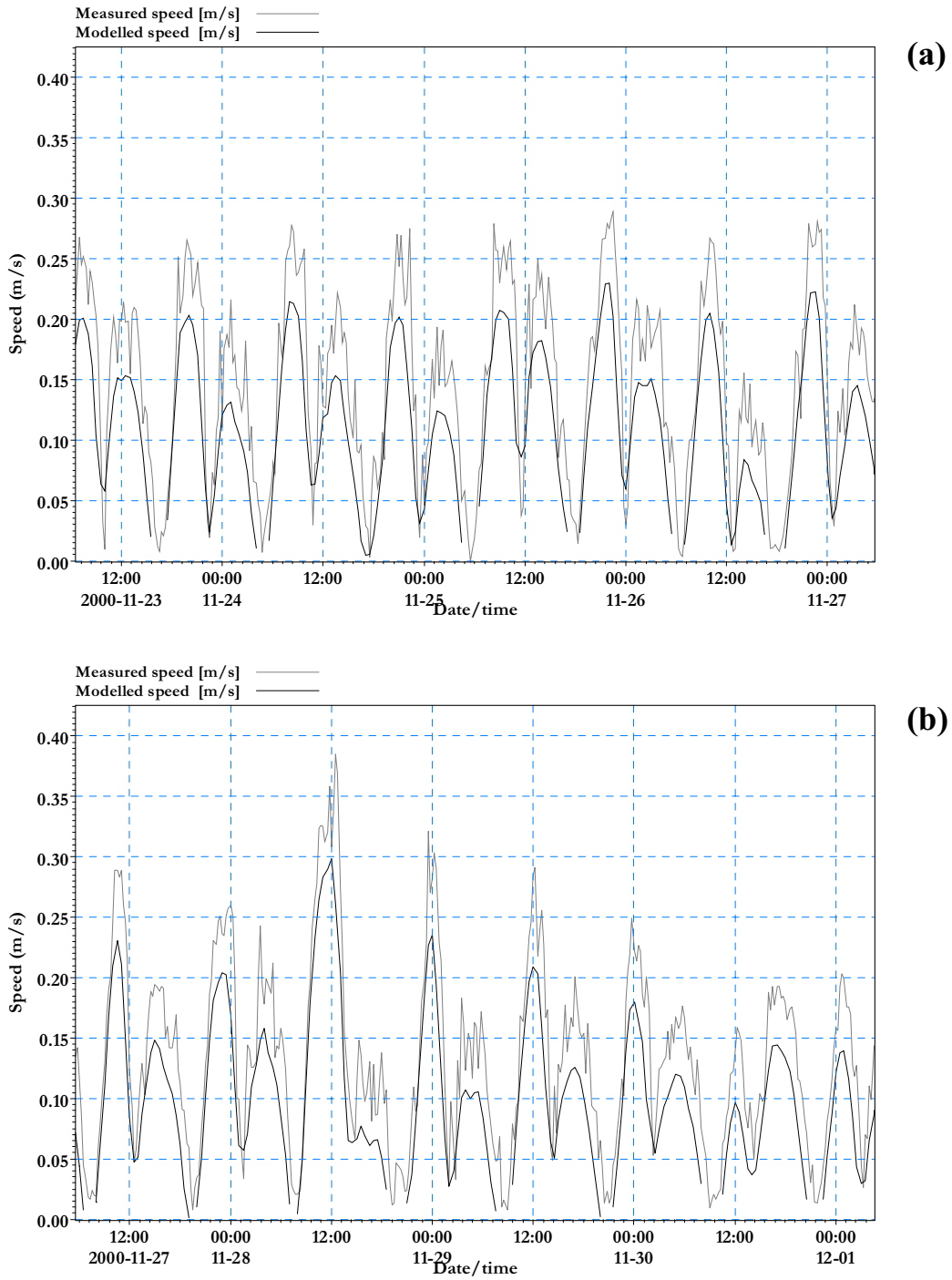

Figure 21:

Time-series of predicted and measured currents at Cockle Bay between (a) 1st and 5th of December 2000 (b) and 5th and 9th December 2000.

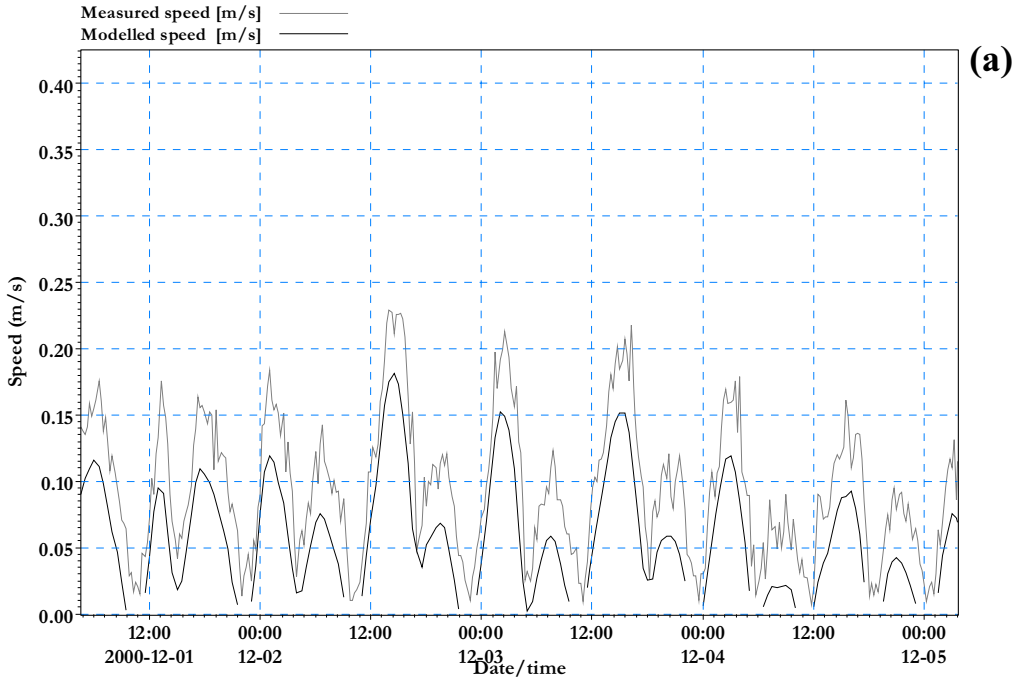

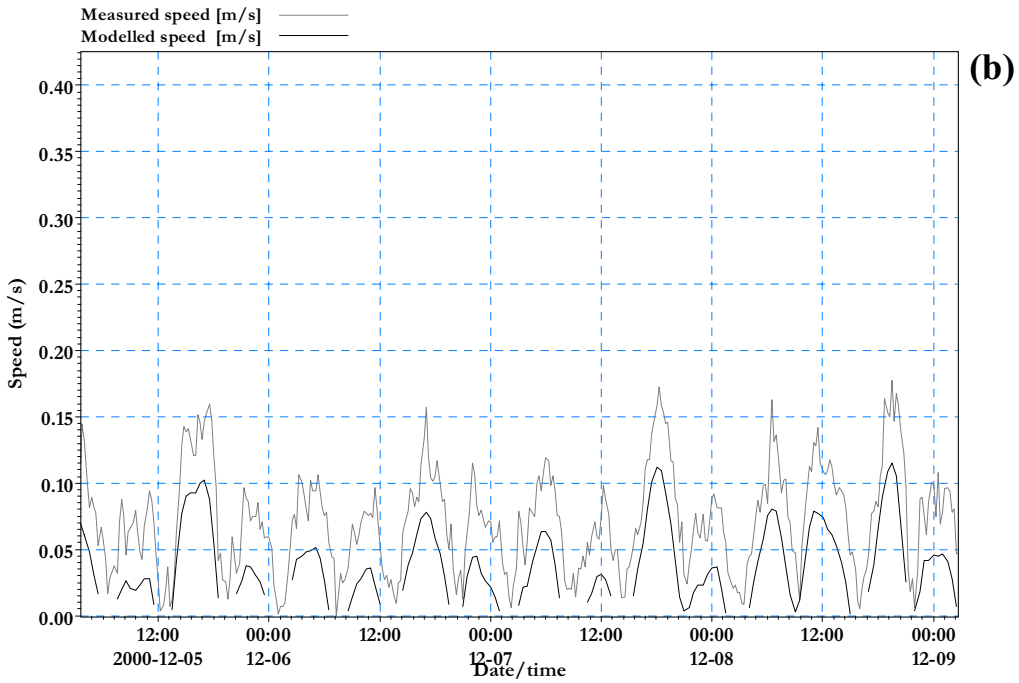

Figure 22:
Regression of measured and predicted current speeds at Cockle Bay (near Mangamangaroa Inlet) for the period between the 21st of November and the 10th of December 2000.

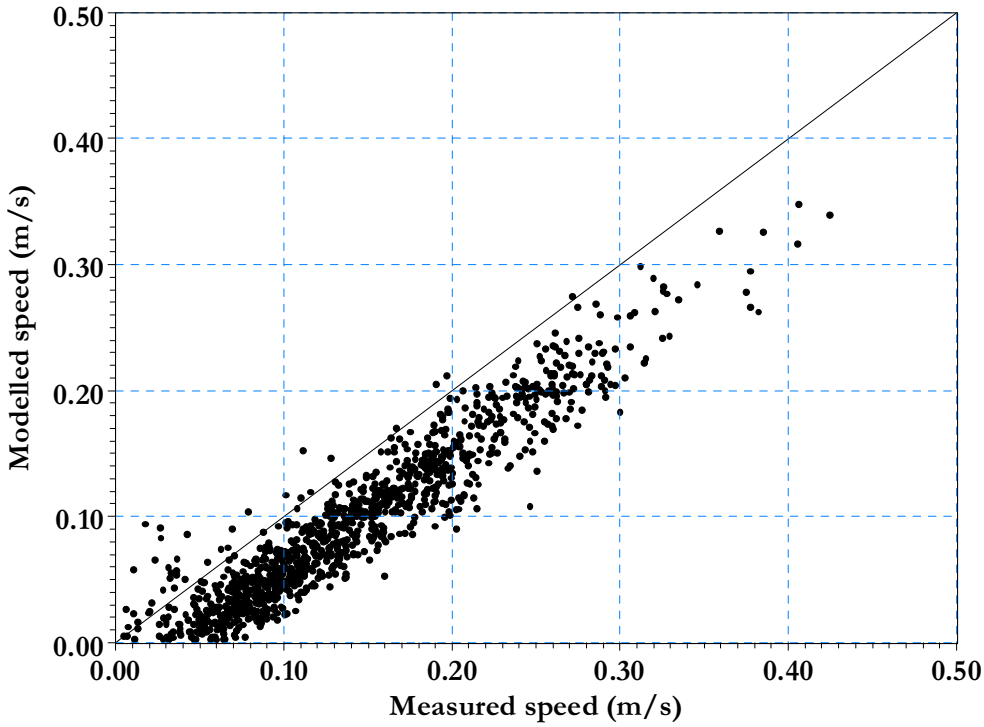

4.4 Baroclinic calibration

One of the major factors influencing the spread of plumes within the coastal environment is the vertical and horizontal mixing coefficients, which can vary depending on the length scales of the plume dimensions. When it comes to modelling the mixing characteristics of a plume on a discrete model grid, the mixing coefficients need to be appropriate for the grid scale being used. For the model simulations of larger-scale plumes performed in this study, a vertical dispersion value of 8×10-4 m2/s was employed. This value is at the lower end of the range of vertical mixing coefficient values measured during several field studies in coastal areas of the North Sea (ranging from 9×10-4 to 63×10-4 m2/s) obtained by Morales et al. (1997). However the field measurements within the Gulf (Bell et al., 1999) derived vertical mixing rates of 1×10-5 m2/s (for scenarios involving low wind speeds). The use of lower mixing rates is more conservative as it curtails plume spreading and thus gives lower dilution rates than might otherwise be the case. For the horizontal mixing coefficients a value of 0.15 m2/s was employed for the 100 m grid. This is in keeping with other studies carried out by NIWA within the Hauraki Gulf (Oldman & Black 1997, Green et al. 1999, Green & Oldman 1999, Oldman & Swales 1999, and Oldman and Senior 2000).

The calibration/verification at this stage has established that the model can accurately model the rise and fall of the tide within the RHM domain and that it can adequately (within the limitations of a 100 by 100 m grid) simulate the tidal and non-tidal currents. The next stage of the modelling process is to check the ability of the model to simulate mixing processes for discharges and flows of different density water masses. Mixing or dispersion is a combination of advection (brought about by the main large-scale currents) and diffusion (i.e. plume spreading due to buoyancy of lighter water masses and smaller scale turbulence, e.g., small eddies and wind-wave motions). Plume advection is determined primarily by the currents so that given a well calibrated hydrodynamic model the advection of a plume will be well simulated. Of equal importance is the rate at which the plume diffuses – a point source discharge in still water will spread at a rate determined by both the plume characteristics (density, temperature, discharge speed and volume) and the ambient water conditions such as water-column density stratification and the degree of turbulence.

Calibration of a dispersion model can be done against field measurements of salinity (a measure of how fresh and saline waters mix), tracking a dyed discharge (a direct measure of near-field and far-field dilution), temperature (measurement of how waters of different density mix), and suspended sediment (measurements of sediment plume concentrations). The latter measurements become more complex because of settling and resuspension processes.

4.4.1 Temperature – Firth of Thames

To show the capabilities of the model to simulate dispersal we have taken temperature data from Firth of Thames mooring in 1999 – 2000 and compared with model results. One process which is very important in terms of water-column temperature structure is stratification. Stratification is the tendency for the water column to develop horizontal layering of different densities due to thermal heating or freshwater river inputs with the lightest water at the surface. Under the right meteorological and oceanographic conditions the temperature structure throughout the water column becomes self-sustaining in that the density structure helps maintain the temperature structure. This stratification is often broken down by storm events (which increase vertical mixing) or the intrusion of waters from outside the region being considered. Modelling of such stratification events means the model must simulate the horizontal and vertical mixing and advection of "remote waters" under different meteorological and oceanographic conditions.

From the Firth of Thames data two periods were chosen. The first included a break down, and subsequent build up of water-column stratification (March 2000), and a second period (September 1999) where there was a slow build up of water-column stratification over a period of 3 weeks. Figure 23 shows the measured and predicted temperatures for the March 2000 period and Figure 24 shows the data for September 1999. The comparisons show that the RHM picks up the overall pattern of temperature stratification in the Firth of Thames

Figure 23:
Model comparison to the Firth of Thames mooring data (March 2000) showing the good match between observed and modelled temperature stratification.

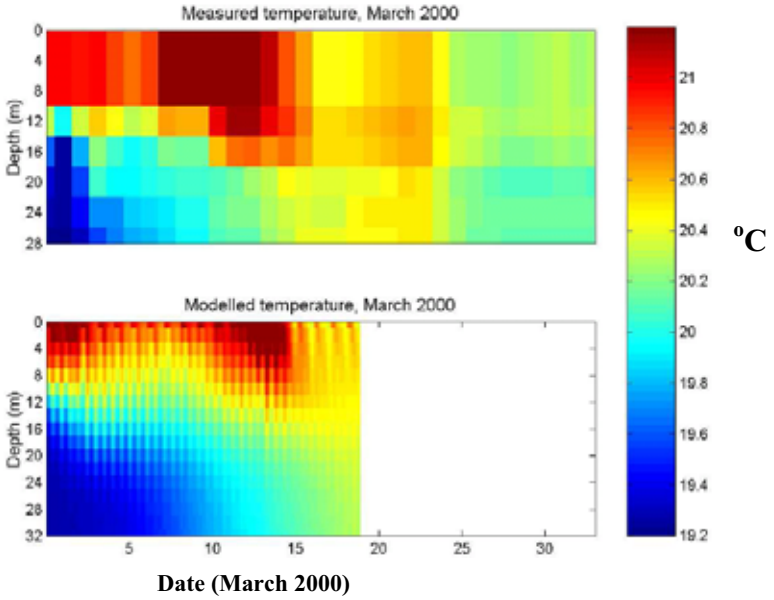

Figure 24:
Model comparison to the Firth of Thames mooring data (September 1999) showing the good match between observed and modelled temperature stratification.

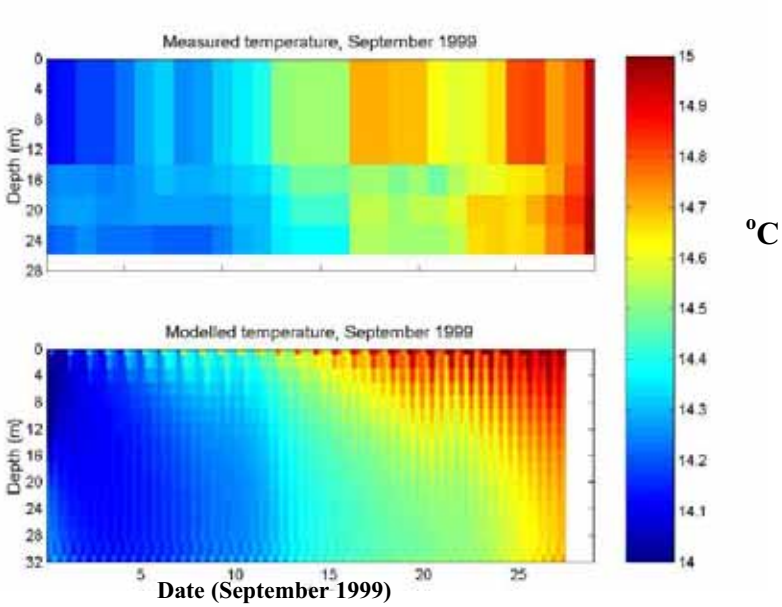

4.4.2 Salinity – Waitemata Harbour

A second simulation was carried out to determine the ability of the model to predict salinity variations (essentially large-scale plume behaviour) within the Waitemata.

Salinity data collected at the entrance to the Waitemata by Metrowater Ltd was used to verify the model for a period when a number of smaller inflow events occurred (Figure 25). This inflow data was derived as part of the hi-resolution case study (Oldman et al, 2004b). At each of the sites shown in Figure 26 the time-series of inflows from the Eastern Bay site was scaled according to the magnitude of the average inflow at each of the sites as shown in Figure 26. The boundary salinity was set to 32.7 (based on Practical Salinity Scale, PSU), while the inflow salinity was set to 12. Based on the predicted tides and observed winds for the period of the deployment the model was run for a period of 14 days. Figure 27 shows the resulting predictions for the last 6 days of the simulation (when the inflow events occurred). Note that the vertical lines in the field data indicate periods where there is missing data. Overall the model tracks the changes in salinity throughout the tidal cycle (both in terms of the phasing and high and low water salinities) and over the period of the inflow events. Low water salinities (lowest values) are well matched throughout the simulation. This indicates that the dispersal of the freshwater inflows on the falling tide are being modelled well. The model tends to slightly over predict the high water salinities (highest values on each tide) towards the end of the simulation. This indicates that there may have been a slight downward trend in inner Gulf salinities during the period of the calibration which cannot be accounted for without actual measurements. A summary of the percentage fit for the various calibration data is presented in Appendix 1.

Figure 25:
Freshwater inflows to the Eastern Bays and entrance to the Waitemata Harbour

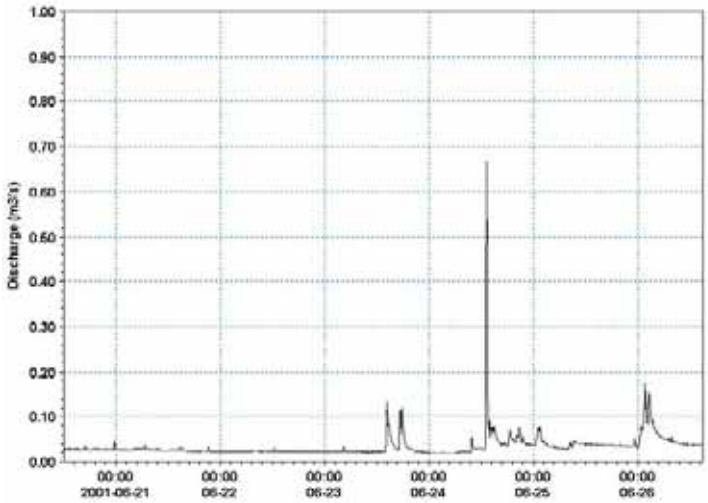

Figure 26:
Relative magnitude of other freshwater flows to the RHM for period of salinity calibration.

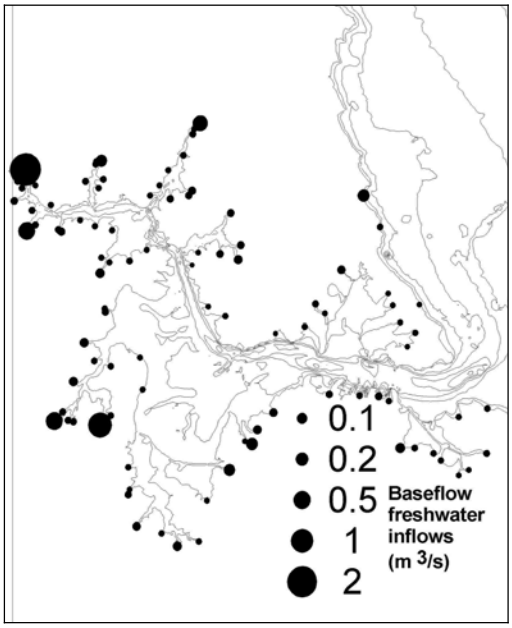

Figure 27:
Modelled and measured salinity data fro the period 21st to the 26th of June 2001. Vertical lines in the field data show periods of missing field data.

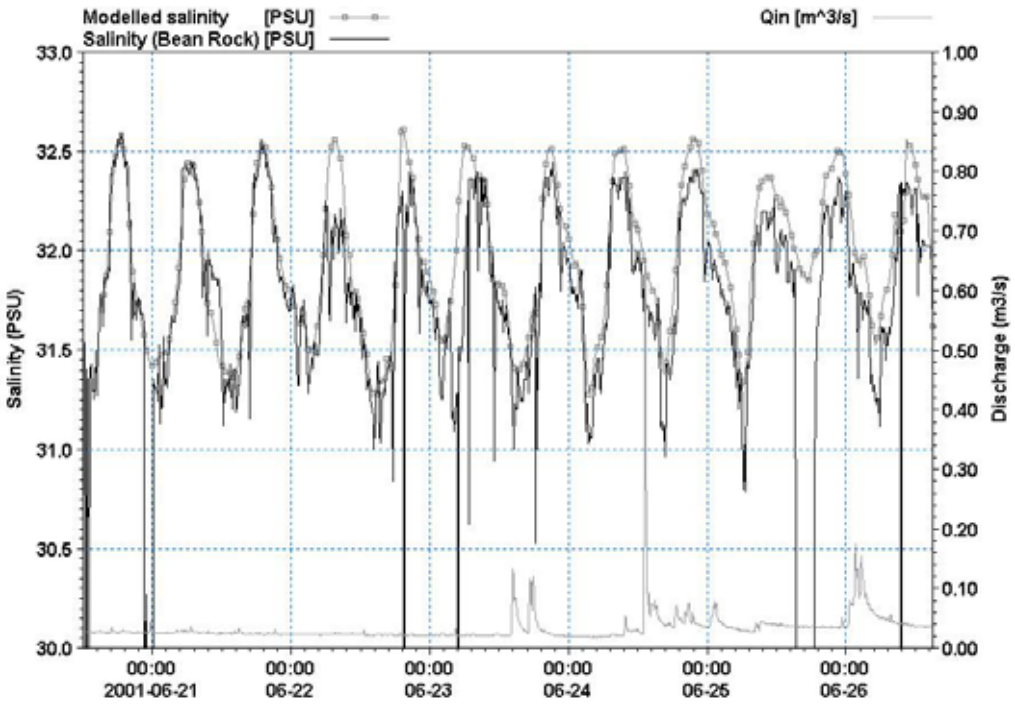

5 Schematic model runs

5.1 Introduction

The initial development of the RHM also included the running of a number of baseline simulations to provide a baseline dataset for future use of the RHM. These simulations included:

- Neap tide with calm conditions and 90th percentile wind velocity from the NE, SE, SW and NW based on the Whangaparaoa automated weather station;
- Spring tide with calm conditions and 90th percentile wind velocity from the NE, SE, SW and NW (again based on the Whangaparaoa automated weather station);
- Highest astronomical tide with calm conditions.

5.2 Model run details and results

Tidal constituent data along the northern boundary of the model were used to define the neap, spring and HAT tide levels for the schematic model simulations. Table 11 gives the average values for tide heights along the whole of the boundary. From the long-term wind record at the Whangaparaoa AWS (Figure 28) the 90th percentile wind speeds from each quadrant (NE, SE, SW, NW) were derived (Table 12). Wind velocities (W) were converted for modelling purposes to an equivalent 10-m height reading W_{10} in oceanographic convention (i.e. "blowing to") assuming the empirical altitude relationship:

$$\frac{W}{W_{10}} = \left(\frac{z}{10}\right)^{k} \qquad (1)$$

where z = anemometer height (m) and k varies with atmospheric stability with a typical value of 1/7 (Beer, 1997). For comparison, the outer Hauraki Gulf values from the Mokohinau Islands automated weather station are also presented in Table 12.

Using these boundary conditions and wind values the calibrated model was use to simulate each combination of tide range and wind conditions. The figures in Appendix 2 show the output from the model summarised in the form of a water level plots (high and low water) and peak velocities (ebb and flood tide).

Table 11:

Mean tidal information (averaged along the northern boundary of the RHM) for schematic model conditions.

Tidal condition	Low water (m)	Mean sea level	High water (m)
Neap tide	0.69	1.66	2.63
Spring tide	0.36	1.66	2.96
HAT	0.03	1.66	3.29

Table 12:

90th percentile wind speeds (10 m above sea level) based on 17-year wind record from the Whangaparaoa AWS. For comparison the equivalent values from the 23-year wind record from the Mokohinau Islands automated weather station are provided (in brackets).

Wind direction	90th percentile wind speed (m/s)	Percentage of time from quadrant (%)
NE	14.8 (16.7)	21 (17)
SE	14.1 (18.0)	16 (20)
SW	12.7 (16.0)	34 (36)
NW	12.7 (17.3)	30 (27)

Figure 28:

(a) Wind rose for Whangaparaoa AWS (corrected to 10 m above sea level) from 17-years of wind record (1986 –2004) and (b) the equivalent from the 23-year record from the Mokohinau Islands AWS. Wind speed is in m/s.

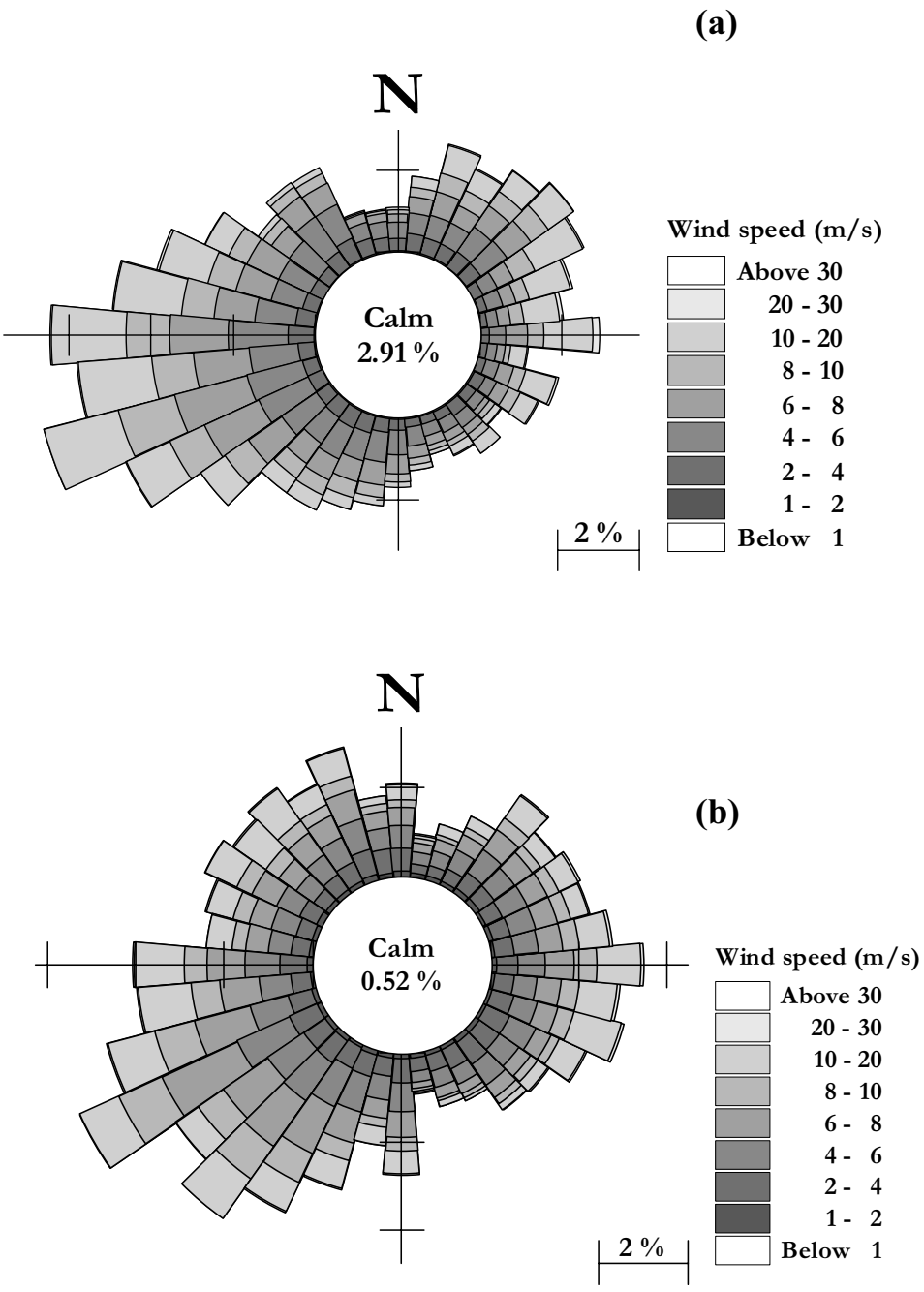

6 Conclusions

A regional harbour model (RHM) has been set up for the inner Hauraki Gulf and associated harbours, to provide a consistent and reliable framework to assist future assessments of the environmental effects of discharges to the marine environment.

The RHM has been calibrated and verified against appropriate available field data. This process has included comparing model predictions of water levels, tide ranges, tidal currents and temperature stratification, against actual field measurements.

One outcome of the work has been to identify the lack of synoptic data relating to the point source discharges of stormwater into the receiving environment of the Inner Gulf. Collection of such data (i.e. simultaneous measurements of source discharge and water quality and its subsequent dispersal and related sediment deposition) would provide further verification of the model.

Calibration and verification of tidal levels provided a good match between observed and predicted water levels across the entire model domain.

Calibration and verification of tidal currents ellipses and currents provided a reasonable match between observed and predicted. Calibration of tidal currents is generally more difficult because current velocities vary spatially much more than the more slowly changing tidal water levels. Consequently, obtaining a good match between modelled current velocities and field measurements at a point is much more dependent on the spatial grid resolution of the model. For example, the RHM comparisons are between field measurements collected at a particular location, depth, and time whereas model predictions are for currents averaged over time, distance and depth (i.e. 100 m by 100 m grid cells in the horizontal and 2 m depth layers). Calibration of tidal currents (and dispersal models which suffer the same constraints) normally improves considerably by using a higher resolution model grid that reflects the spatial variation of the current velocity and mixing processes being modelled. This is achieved using a nested model grid within the RHM centred on the specific area of interest.

Calibration of the dispersal model for large-scale plumes and mixing behaviour has shown that temperature variations due to thermal mixing of oceanic (i.e. outer Gulf) and estuarine waters (i.e. Firth of Thames) are predicted well by the model. In combination, advection, horizontal and vertical mixing processes are well represented within the model. The mixing of catchment-derived freshwater inflows to the Waitemata Harbour and saline waters of the inner Gulf are also being modelled accurately, further confirming the ability of the dispersion model to simulate the mixing processes at length scales of 100 m or more.

A series of initial baseline tide, wind and stratification scenarios have been run to provide a baseline dataset for future use of nested models within the RHM. Nested models need to be at a 1:3 ratio of 100 m (i.e. 33 m, 11 m grid cells). These higher-resolution nested models will provide a closer match to point-velocity measurements and small-scale plume behaviour than the baseline 100 m model.

7 References

Beer, T. 1997: *Environmental oceanography.* 2nd edition. Boca Raton, Florida, CRC Press Inc. 367 p.

Bell, R.G.; Oldman, J.W.; Turner, S.J.; Gibbs, M.M.; MacDonald, I.; Mills, J. (1999). Oceanographic and water quality investigations for the North Shore City outfall: Assessment of environmental effects. NIWA Client Report: NSC90201/3.

Black, K.P., Bell, R.G., Oldman, J.W., Carter, G.S & Hume, T.M. (2000). *Features of 3-dimensional barotropic and baroclinic circulation in the Hauraki Gulf, New Zealand*. New Zealand Journal of Marine and Freshwater Research. Vol 34, 1-28.

Green, M.O.; Oldman, J.W. (1999). Deposition of flood-borne sediment in Okura estuary. NIWA Client Report: ARC90242/2.

Green, M.O.; Stroud, M.J.; Oldman, J.W.;Senior, A.K.; Cooper, A.B. (1999). Long Bay Sedimentation Study: Stage I (Sediment Generation) and Stage II (Sediment Fate). NIWA Consultancy Report NSC00209

Morales, R.A.; Elliott, A.J.; Lunel, T. (1997). The influence of tidal currents and wind on mixing in the surface layers of the sea. *Marine Pollution Bulletin 34(1)*: 15–25.

Oldman, J.W.; Senior, A.. (2000) Wilson Bay Marine Farm Dispersal Modelling NIWA Client Report: EVW01218

Oldman, J.W.; Black K.P. (1997). Mahurangi estuary numerical modelling. NIWA Client Report: ARC60208/1

Oldman, J.W.; Swales, A. (1999). Mangemangeroa estuary numerical modelling and sedimentation. NIWA Client Report: ARC70224.

Senior, A., Oldman, J.W., Green, M.O., Norkko, A., Hewitt, J., Collins, R.P., Stroud, M.J., Cooper A.B., Thrush, S. (2003). *Risks to estuarine biota under proposed development in the Whitford catchment.* NIWA Client Report No. Ham2003-016. August 2003.

Walters, R.A.; Goring, D.G.; Bell, R.G. (2001). *Ocean tides around New Zealand*. NZ Journal of Marine and Freshwater Research. 35(4): 567-579.

Water Quality Centre (1992). *North Shore outfall oceanographic survey: Current meter deployments, April-May 1992*. Water Quality Consultancy Report No. 6143/1 prepared for Beca Steven and North Shore City. DSIR, Hamilton.

8 Appendix 1

Percentage fit for the various calibration data presented within the report.

Error	Salinity calibration	Tidal constituent height	Tidal constituent current	Red Bluff currents	Cockle Bay currents	Whitford water levels
< 5%	94.8658	37.5	0.000	5.2371	0.8357	19.1667
5-10%	1.7503	18.75	14.2857	10.4388	2.4141	33.8889
10-15%	0.4667	31.25	50.0000	10.0495	3.0641	19.0278
15-20%	1.0502	6.25	7.1429	8.6341	4.0854	9.5833
20-25%	0	6.25	14.2857	8.0326	5.7567	4.8611
20-25%	0.1167	0	7.1429	7.5018	7.5209	2.3611
25-30%	0	0	7.1429	5.8740	7.5209	1.2500
30-35%	0	0	0	4.2109	6.7781	1.9444
35-40%	0	0	0	4.2817	6.0353	0.6944
40-45%	0.1167	0	0	3.3970	6.1281	1.1111
>50%	1.6336	0	0	32.3425	49.8607	6.1111

9 Appendix 2

Water level plots (high and low water) and peak velocities (ebb and flood tide) for schematic model runs for various tide and wind conditions of the RHM.

Calm conditions

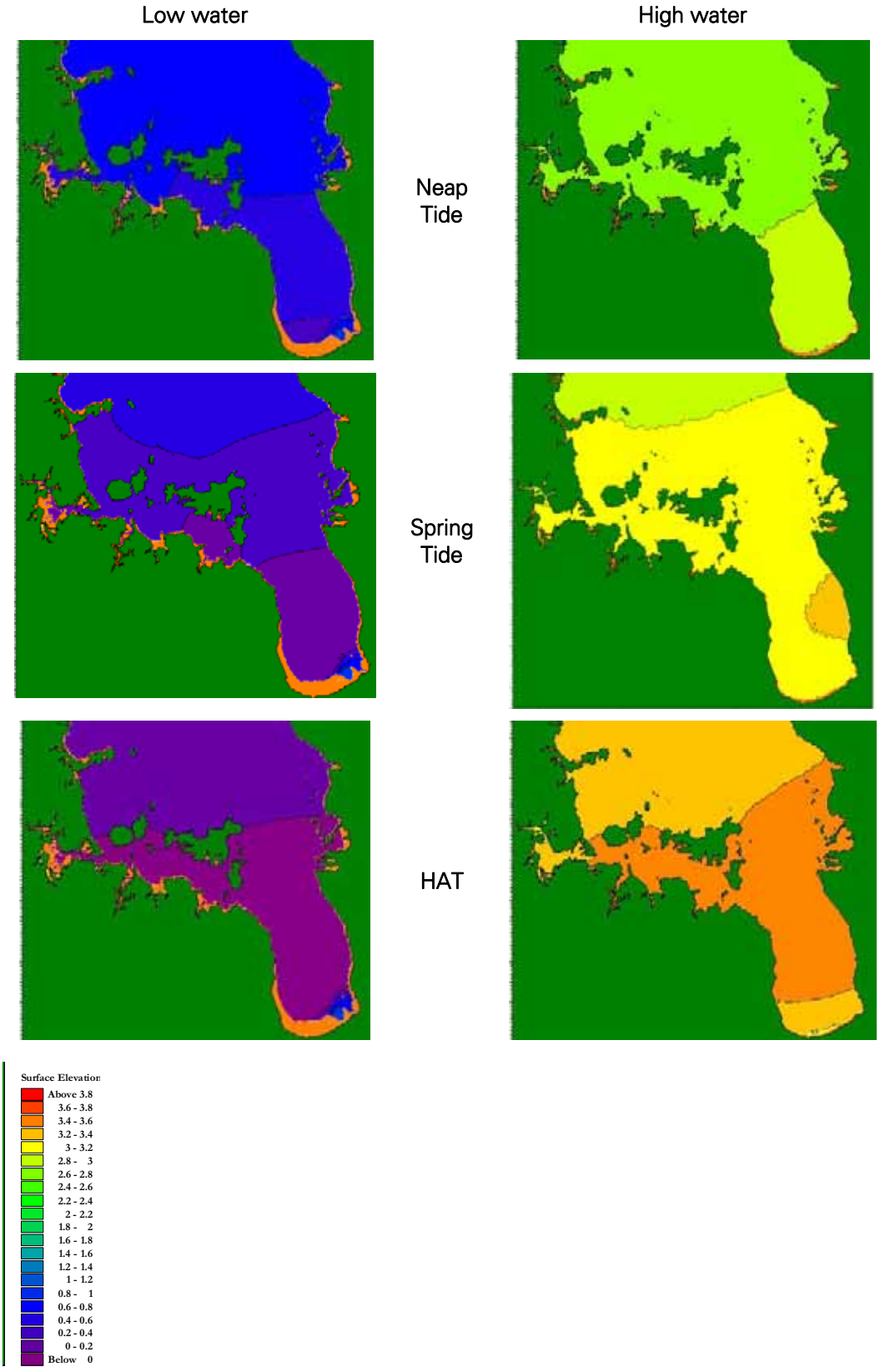

North East Winds

Low water

High water

Neap Tide

Spring Tide

HAT

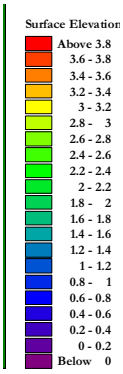

South East Winds

Low water

High water

Neap Tide

Spring Tide

HAT

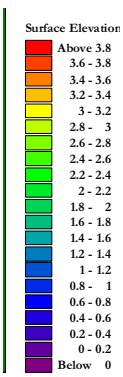

South West Winds

Low water

High water

Neap Tide

Spring Tide

HAT

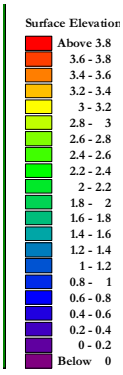

North West Winds

Low water

High water

Neap Tide

Spring Tide

HAT

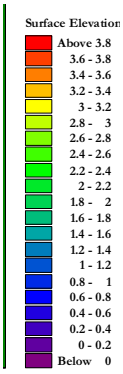

Calm conditions

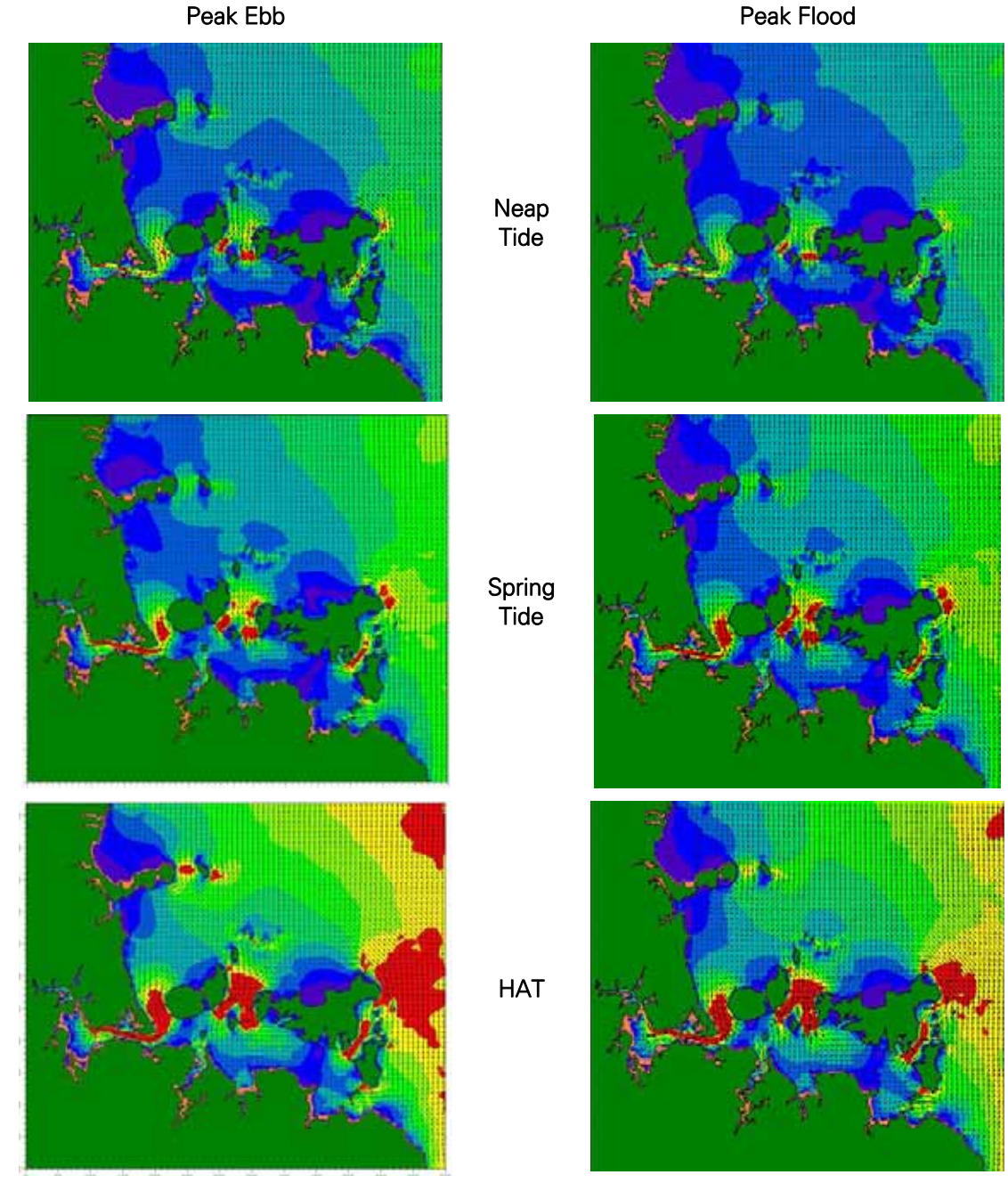

North East Winds

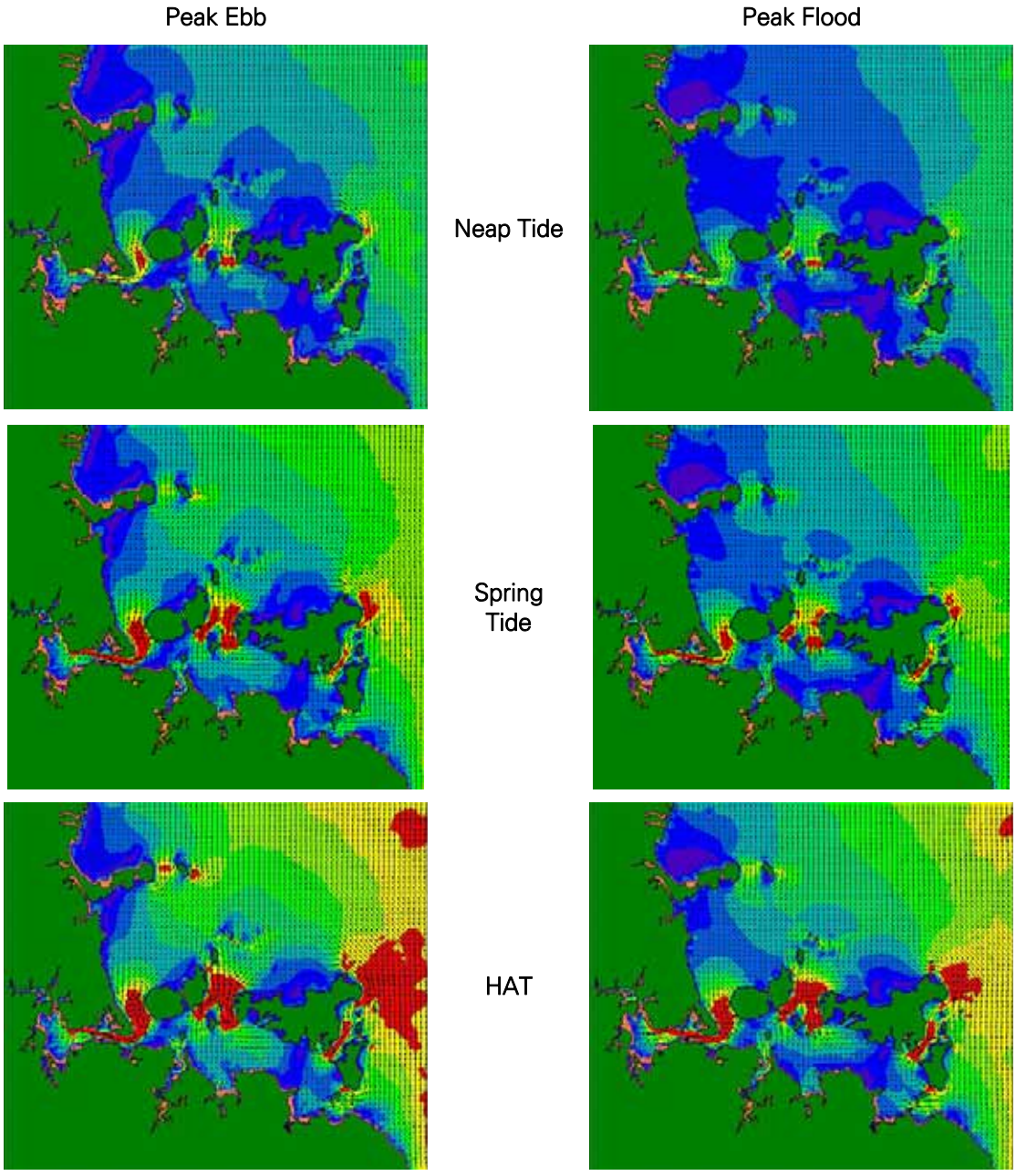

South East Winds

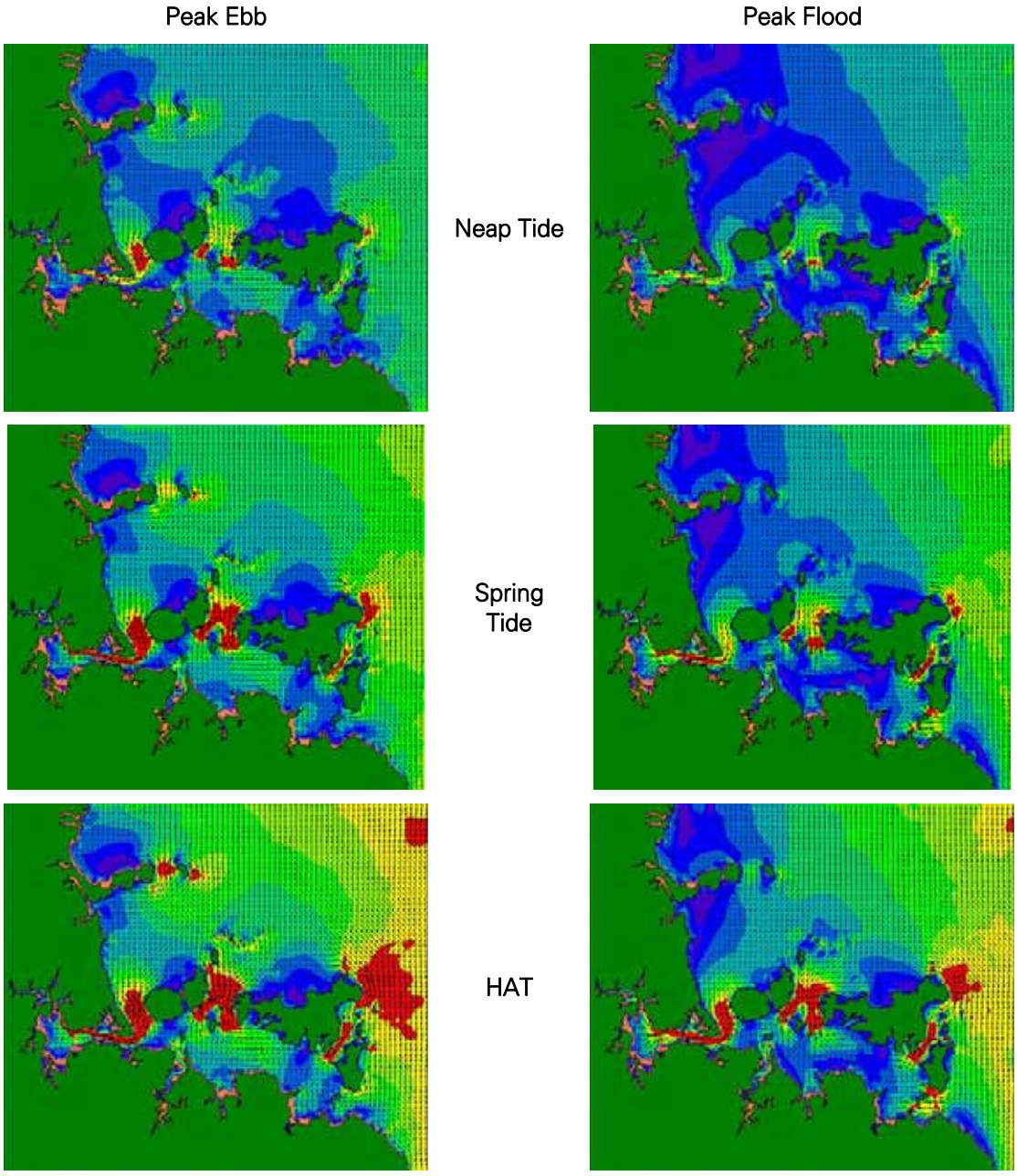

South West Winds

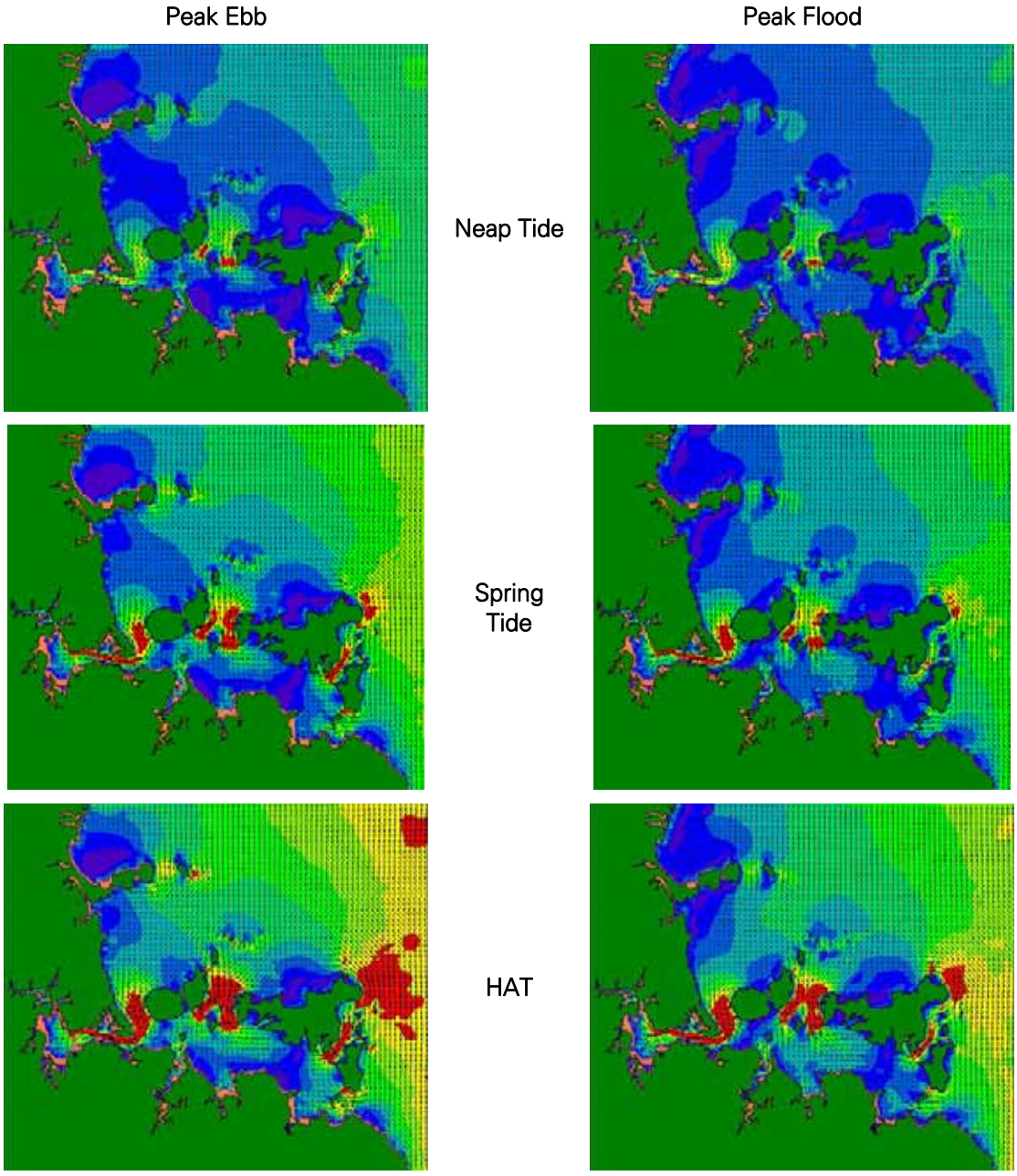

North West Winds

Peak Ebb
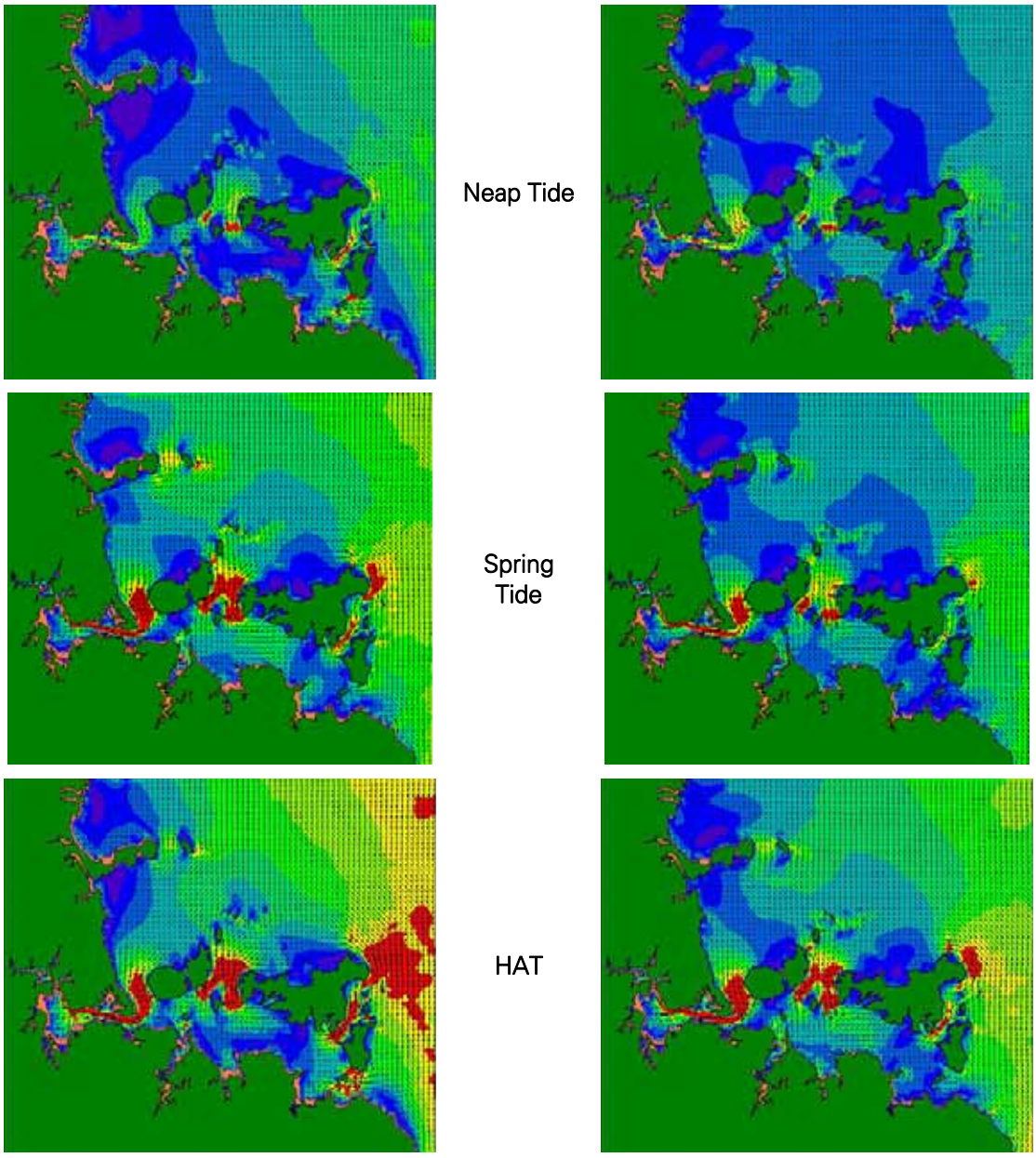
Peak Flood